UNITED NATIONS UNIVERSITY
UNU-GTP
Geothermal Training Programme

Orkustofnun, Grensasvegur 9,
IS-108 Reykjavik, Iceland

Reports 2017
Number 27

RESERVOIR ENGINEERING DATASETS AND SIMPLE MODELLING IN EARLY STEAMFIELD DEVELOPMENT

Arief Imam Santoso
Directorate of Geothermal
Directorate General of New, Renewable Energy and Energy Conservation
Ministry of Energy and Mineral Resources
Jl. Pegangsaan Timur No 1, Menteng,
Central Jakarta
INDONESIA
ariefisantoso@gmail.com

ABSTRACT

In order to expedite development of the Indonesian geothermal potential, the government plans to drill deep exploration wells before tendering out new geothermal working areas. Success of such activities is subject to the proper location of the exploration wells and thorough testing of the wells during drilling, recovery and testing. Reservoir engineering datasets comprise a large fraction of these data and their analysis is the subject of this report. Volumetric models being developed at the surface exploration stage can give an indication of the power potential at hand. Here a few examples are given, from three different countries. The Corbetti resource in Ethiopia, infers a reserve area of 50-100 km^2, 1-2 km of thickness and 260-360°C temperature. A Monte Carlo based volumetric model for these parameters yields a probable generating capacity at or above 970 MWe. Similarly, the already drilled Rantau Dedap resource in Indonesia is characterized by 3-17 km^2 of a 1.3 km thick reservoir at 230-290°C. This yields some 50 MWe of proven generating potential using the volumetric model approach and a single-flash heat to power conversion. A bottoming binary system may provide another 25 MWe. Example can also be taken from Iceland. Analysis of downhole pressure and temperature data in a 2500 m deep well SV-26 in Svartsengi, Iceland, results in a static water table at 425 m, a boiling point with depth zone to 700 m, and near isothermal 240°C single-phase water reservoir to total depth. Two major feedzones are identified at 1225 and 2200 m TVD (total vertical depth) and the well pressure pivot point is located at 1350 m TVD and at 77 bar-g. Multistage injection and production test analysis result in a cold well injectivity index of 11 kg/s/bar and a hot well productivity index of 28 kg/s/bar. Both indicate a very good reservoir. Detailed hydrological models of injection and production transient pressure data show well skin in the negative territory and reservoir permeabilities in the 10-1000 mD range. Higher model values arise from models calibrated against well data collected before running the 7” slotted liner. This may suggest that the lower cold water injectivity index relates to liner holes viscosity effects. A numerical flowing wellbore model was able to capture these properties; the bottomhole and wellhead pressure with flow and the dynamic temperature and pressure profiles with depth. The model predicts a shallow to deep feedzone ratio at 2:1. The modelled wellhead output curve infers a much higher maximum flowrate than the tested maximum of 47 kg/s, thereby taking well capacity close to 10 MWe.

1. INTRODUCTION

Indonesia is a country that is known for its abundant geothermal potential. Located in the Pacific ring of fire belt, which extends from Sumatera to Maluku, Indonesia is estimated to contain over 11 GW of geothermal resources and 17.5 GW of geothermal reserves. Although it has a large potential and the development started in the early 1970s, currently, Indonesia only utilizes the geothermal potential for a 1.6 GW electrical capacity or about 10% of its reserves. The current installed capacity is still far from Indonesian government's target to reach 7.2 GW of geothermal electricity in 2025 (Ministry of Energy and Mineral Resources, 2017).

To accelerate the geothermal development, the Indonesian government has made some measures, which include the changing of geothermal regulations with the establishment of law no. 21/2014. One of the important elements of the new law is that the government is allowed to develop geothermal areas through exploration to the exploitation stage. To support the plan, the government also provides a geothermal fund, which comes from the national budget (Ministry of Energy and Mineral Resources, 2017).

The World Bank is an international institution that supports the development of renewable energy in many countries including Indonesia by providing additional funds through the Geothermal Energy Upstream Development Project (GEUDP). The project provides a revolving fund, which consist of 49 million USD for exploration funds and 6.75 USD for technical assistance. The project includes many elements from the Indonesian government such as Directorate of Geothermal and Geological Agency of Ministry of Energy and Mineral Resources and Ministry of Finance. PT Sarana Multi Infrastruktur (PT SMI), a state-owned company, will also participate as the fund holder (The World Bank, 2017).

The government's drilling project started with preliminary environment and social surveys of five promising geothermal areas. It was finally decided that Waesano in East Nusa Tenggara will be the first area where drilling will take place through the government exploration drilling scheme. Currently, the project has finished its Environmental and Social Impact Assessment (ESIA) and will begin scouting for drilling contractors (Ministry of Energy and Mineral Resources, 2017).

As the government will become one of the decision makers in every aspect including well targeting, drilling mechanism, etc., knowledge and competence in geothermal development are important to support the decision making. This paper will discuss datasets of reservoir engineering that assist in producing a qualified decision. The reservoir engineering datasets studied here will include a resource assessment of two different stages of geothermal development, one in the early exploration stage with complete geoscience surveys in Corbetti, Ethiopia and one in later exploration stage with exploration wells already been drilled in Rantau Dedap, Sumatera, Indonesia. It will then be continued by well-testing analysis to obtain reservoir properties from pressure and temperature logging, and multistage injection and production tests from well SV-26 in Svartsengi, Iceland. The final part of the project will be a wellbore simulation to generate the output deliverability curve and contribution ratio of feedzones.

2. LITERATURE REVIEW

2.1 Resource and reserves of geothermal reservoir

Geothermal potential can be classified into a few categories. According to Muffler and Cataldi in 1978, a geothermal resource is thermal energy that is stored between the earth's surface and a certain accessible depth, which is shallow enough to be extracted by drilling. It should also be possible to extract this thermal energy legally and economically for a certain amount of time (Sarmiento et al., 2013). Dickson and Fanelli (2004) also provide another definition by stating that reserves are a part of the resources that could be extracted economically compared to other energy sources and it is characterized by drilling or by geological, geochemical and geophysical data.

Geothermal reserves are then classified based on the reasonable certainty of how much of the thermal energy can be extracted from the system. In 2013, Sarmiento et al. mentioned three categories of reserves based on this as shown in Figure 1. These are defined as possible, probable and proven reserves. The proven assessment can only be achieved with deep exploration drilling while the possible and probable reserves are largely based on indirect stored heat assumptions from surface work.

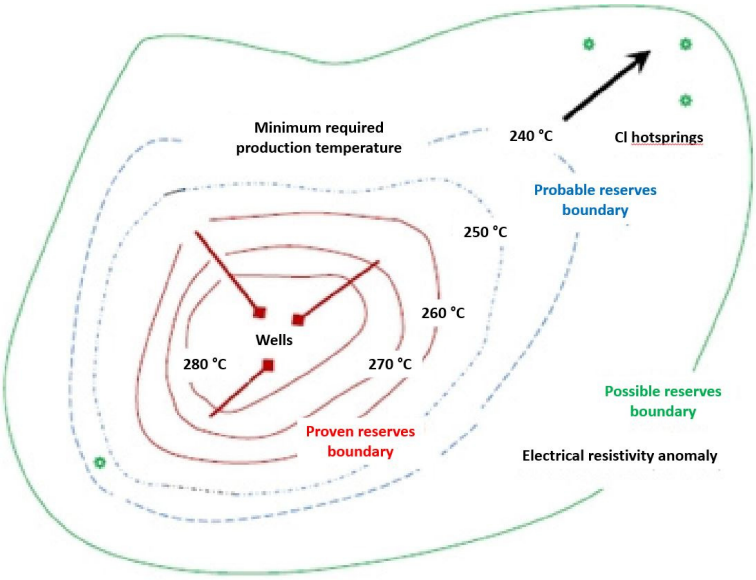

FIGURE 1: Illustration of the boundaries used in differentiating the three different types of reserves (Sarmiento et al., 2013)

2.1.1 Possible reserves

Possible reserves are the category that has the least field data support for estimating the heat reserve at depth compared to the other reserves categories. The determination of the reserves is based on surface exploration such as the existence of surface manifestation (hot springs, fumaroles, etc.) and its geochemistry analysis, resistivity anomalies, etc. In this category of reserves, the surface area of geothermal system is usually determined by the analysis of geophysical resistivity surveys based on methods such as Schlumberger, transient electromagnetic (TEM) or magneto-telluric (MT) measurements. Reservoir temperature for possible reserves calculation is usually based on geothermometers using water, steam and gas from hot springs or fumaroles (Sarmiento, et al., 2013).

2.1.2 Probable reserves

Probable reserves are geothermal reserves that are more likely to be recoverable than possible reserves but less reliable than proven reserves. The surface area of the reservoir is defined by temperature contours based on drilled wells that extrapolate to 240°C to the edge of the field and it also includes area that has extensive surface manifestation where geothermometer results indicate temperatures above 250°C. The reservoir temperature is estimated based on the extrapolation of existing temperature gradient wells or slim hole wells and also chemical geothermometers (Sarmiento, et al., 2013).

2.1.3 Proven reserves

Proven reserves are the portion of the resource that can be extracted with reasonable certainty based on geoscience and engineering data. Compared to other categories, proven reserves have the best probability and certainty because the reserves estimation is usually based on more reliable data, such as from drilling and well logging. The surface area for the estimation is based on production wells that are hot enough to be able to produce power from a commercial perspective (Sarmiento, et al., 2013). Unlike probable and possible reserves, reservoir temperature for proven reserves is obtained from direct measurement of the wells instead of geothermometers or extrapolation from shallow wells.

2.2 Volumetric calculation

One of the most important steps before deciding to develop a potential geothermal area is doing a volumetric resource assessment. Geothermal resource assessment is done by estimating the energy that

could be extracted from a certain geothermal reservoir to be utilized in a sustainable way for a long time period. The estimation is based on all gathered information such as geoscientific data from early exploration surveys or downhole data after wells have been drilled (Sarmiento et al., 2013).

Resource assessment can be done in various stages of geothermal development. In each stage, there is a certain resource assessment suitable for the estimation. For example, in early development when the field data is based on surface geoscientific surveys only, a volumetric calculation with the Monte Carlo simulation technique is the best option for resource assessment. Volumetric assessment is done with a calculation of thermal energy that is stored in the rock and fluid and how much of that energy could be extracted for further utilization (Sarmiento et al., 2013).

Essential volumetric model parameters are based on the analysis of all available data, such as geological data, geophysical data and sub-surface reservoir temperature that is estimated with geothermometers. These are gathered to build a conceptual model of the reservoir. A conceptual model is a descriptive and qualitative model that includes important physical features of the geothermal system and is capable of matching the characteristics intended by the modeller (Grant et al., 1982). The conceptual model is the source of information for the volumetric assessment as it should incorporate all the data that are needed, such as the geological setting of the area, geophysical boundary anomaly, estimated reservoir temperature, estimated thickness of the reservoir and so on. Reservoir properties that are used for volumetric calculation will be discussed in a later section.

As the resource development is progressing, such as when exploration drilling has already been done and relevant reservoir properties have been obtained from the well logging, the conceptual model is continuously updated to accommodate that information. At this point, volumetric calculation is sometimes not the best option for the resource assessment because it treats the geothermal reservoir as a static volume and ignores the recharge of the system. Numerical modelling, on the other hand, is a better option for resource assessment when more significant and reliable data have been obtained. Sarmiento and Björnsson (2007) stated that numerical modelling is a mathematical representation of the physical state of a geothermal reservoir that interprets physical and chemical information from surface and subsurface data. Numerical modelling could also be a reliable method to confirm earlier volumetric calculations.

Reservoir estimation with volumetric calculation depends on various reservoir properties. The parameters that should be considered when doing volumetric calculations are described below.

2.2.1 Reservoir surface area

The determination of the surface area of a geothermal reservoir system is a non-trivial task. The determination has to estimate the subsurface area of the reservoir based only on surface exploration data. It is also especially difficult in a geothermal area which has a complex geological setting (Sarmiento et al., 2013). In the early stage of the development, the surface area is usually based on the area of low-resistivity anomaly resulting from a TEM or MT survey. Such an area is commonly referred to as the top of clay (TOC) anomaly. However, it turns out that the volumetric calculation using the area of low-resistivity is too optimistic and can be several times larger than the actual reservoir area (Cumming, 2016). Therefore, it is usually preferable to use the bottom of clay (BOC) area, which represents the surface area of the top of reservoir (TOR).

With further development of a geothermal field, for example after drilling a handful of exploration and delineation wells, the surface area estimate becomes more confident. However, drilling exploration wells, which can cost 3-8 million USD each, is quite expensive (modified from Sarmiento et al., 2013). That's why the determination of the geothermal area or at least the most plausible area of the reservoir is still important in the early stage. The estimated reservoir surface area is one of the most important parameters to build a conceptual model. With deep wells drilled and downhole reservoir parameters logged directly, the conceptual model is updated for a better understanding of the reservoir system.

2.2.2 Reservoir thickness

Reservoir thickness is another tricky parameter to decide. As in the case for the surface area of a reservoir, it is a subsurface property and its analysis is only based on the surface exploration data before any drilling has been done. The thickness of the reservoir is usually decided from the base of clay cap extended to the depth that is economically feasible to drill with today's technology, at around 3000 m. It is noted that there have been wells that are drilled deeper than this depth, The Iceland Deep Drilling Project in Reykjanes peninsula, for example, has been drilled to reach 4,659 meters depth (Fridleifsson and Elders, 2017). With increasing depth of wells, the permeability of the reservoir decreases and 3000 m depth is usually assumed as the maximum depth where the reservoir fluid can be extracted from (Tulinius, 2017).

2.2.3 Reservoir temperature

The temperature of the reservoir can be estimated in various ways, subject to the development stages of the geothermal area. In the early stage of the development, the temperature estimation is based on geothermometry of fluid samples from hot springs or fumaroles. After some temperature gradient or slim hole wells have been drilled in the area, the temperature estimation can be done with an extrapolation of the temperatures of the wells. At a later stage, the temperature of the reservoir is estimated by a direct measurement of downhole temperature in the producing exploration wells (Sarmiento et al., 2013). In line with the progress of the development, the estimation of subsurface temperature thereby gradually becomes more reliable.

2.2.4 Rock porosity

Rock porosity is a parameter of a geothermal reservoir that is difficult to estimate. In the early stage of development, porosity of the rock matrix of a certain geothermal reservoir is usually determined to be similar to another geothermal area close by. After drilling has been done, the porosity of the rocks can be estimated from the analysis of cuttings and cores. A lithological log with a neutron-neutron log could also be used to determine the porosity of the rocks (Tulinius, 2017). When there is very little data available, usually it is safe to assume the porosity of geothermal area in a volcanic rock matrix to be around 10%.

2.2.5 Recovery factor

Recovery factor is the fraction of how much of the thermal energy stored in the fluid and rock matrix of the geothermal reservoir can be extracted to the surface. The recovery factor is dependent on the permeability (Sarmiento et al., 2013). Muffler and Cataldi (1978) make a correlation between porosity of the geothermal rock matrix and the recovery factor by the equation of $R = 2.5\ \varphi$ where R is the recovery factor and φ is porosity.

2.2.6 Rejection temperature

Cut-off temperature or rejection temperature is the limit of how much thermal energy would be utilized from a geothermal reservoir, assuming a certain heat to power conversion technology. Thus, the rejection temperature could be different for different utilizations. For example, the rejection temperature could use the average environment temperature, a minimum temperature for space heating or minimum temperature for electricity generation (Tri Handoko, 2010). The rejection temperature for electricity generation could also differ based on the power plant system used for the utilization. As an example, Sarmiento et al. (2013) suggest to use 180°C for a conventional power plant and 130°C for a binary power plant.

2.2.7 Reservoir fluid properties

The reservoir fluid properties that will be used in the estimation of the reservoir volume are the density of the fluid and the specific heat of the fluid. The specific heat of the fluid that will be used in this calculation is specific heat in constant pressure. Both the specific heat and the density of fluid can be formulated as a function of reservoir temperature where the specific heat will increase with increasing temperature while the density of the fluid will decrease with increasing temperature.

2.2.8 Reservoir rock properties

The properties of rock differ between types of rock. The rock in a geothermal area usually consists of basalt or andesite in a volcanic area and sandstone or limestone in a sedimentary basin. The properties of the rock, which will be used in this calculation are the density of the rock and the specific heat of the rock.

2.2.9 Power plant efficiency

Power plant efficiency is the fraction of the extracted thermal energy from the reservoir, which can be converted into electricity. The efficiency can be estimated in two stages, the first one is the conversion of thermal energy into mechanical energy and then the conversion of mechanical energy into electrical energy. But according to Sarmiento et al. (2013), considering the uncertainties involved in estimating a resource with volumetric calculation, it is sufficient to use a single thermal-mechanical-electrical efficiency for the calculation.

According to Moon and Zarrouk (2012), the efficiency of a geothermal power plant depends on many factors, such as the rejection temperature used in the power plant, the existence of non-condensable gases (NCG) in the geothermal fluid, the amount of energy loss in the pipeline and the efficiency of the turbine and generator itself.

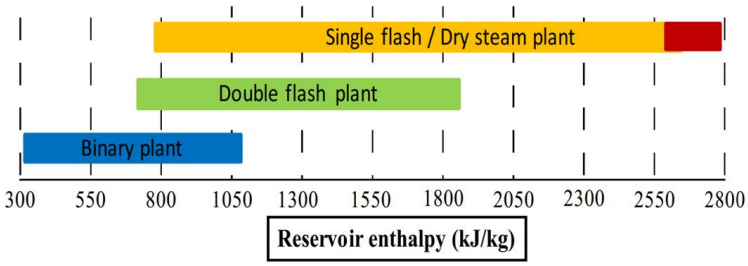

FIGURE 2: Range of enthalpy of operating geothermal power plants based on published data (Moon and Zarrouk, 2012)

Moon and Zarrouk (2012) also make a correlation between the efficiency of the power plant with reservoir temperature and the enthalpy of the geothermal fluid. The decision to choose a certain type of power plant is usually based on the temperature and enthalpy of the geothermal fluid. Figure 2 describes the best power plant option for a certain range of enthalpy.

The efficiency of a power plant differs from one type to another. The relation between the efficiency of a single flash power plant and a binary power plant with temperature is discussed by Moon and Zarrouk (2012) as shown in Figure 3a for a single-flash power plant efficiency vs. temperature and Figure 3b for binary power plant efficiency vs. inlet temperature

2.2.10 Power plant utilization period

The utilization period of a geothermal power plant is usually derived from when the whole investment will be recovered within its target rate of return, usually for 25-30 years (Sarmiento et al., 2013). This could also depend on the prevailing policy of the country where the geothermal area is located. For example in Indonesia the utilization period for a geothermal power plant is assumed 30 years, while in Ethiopia the period is 25 years (Teka Neguisse, EEP, pers. comm., 2017).

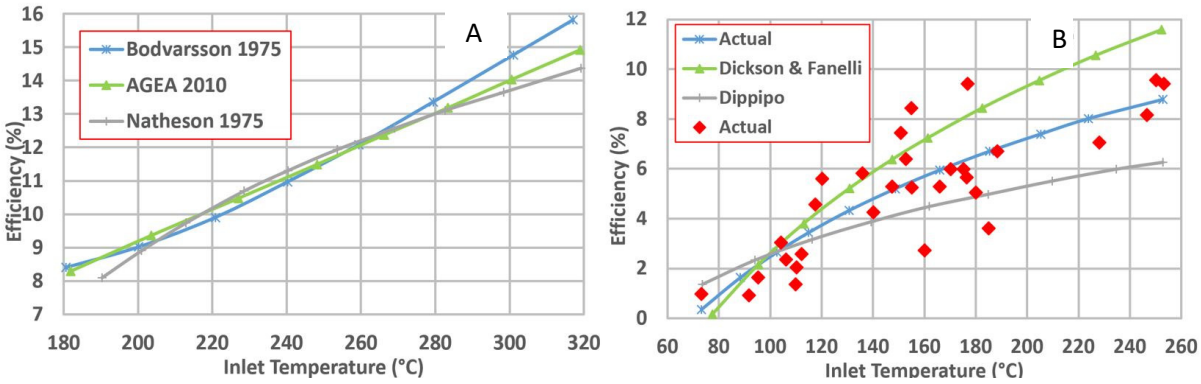

FIGURE 3: a) Efficiency of a single flash geothermal power plant; and
b) Efficiency of a binary power plant (modified from Moon and Zarrouk, 2012)

2.2.11 Power plant load factor

Power plant load factor is the availability of the power plant throughout the years regarding maintenance periods, or whether the power plant is operated at base load or at peak load. The load factor of good operating geothermal power plants around the world ranges from 90 to 97% (Sarmiento et al., 2013).

2.2.12 Governing equation for the volumetric model

The reservoir parameters discussed above are used for volumetric calculation as stated in Equations 1 and 2. The first step of a volumetric calculation is to estimate the total heat (Q_T) stored in the reservoir while the second step is to calculate what fraction of the thermal energy can be recovered and converted into electricity. The parameters used, their symbols and their units are described in Table 1:

$$Q_T = A\ h\ \varphi\ c_f\ \rho_f\ (T - T_r) + A\ h\ (1 - \varphi)\ c_r\ \rho_r\ (T - T_r) \quad (1)$$

$$P = \frac{Q_T\ R\ \eta}{Lf\ t} \quad (2)$$

TABLE 1: Reservoir parameters for a volumetric calculation

Parameter	Symbol	Unit	Parameter	Symbol	Unit
Total thermal energy	Q_T	J	Fluid specific heat	c_f	J/kg°C
Surface area	A	km^2	Recovery factor	R	%
Thickness	h	m	Conversion efficiency	η	%
Rock density	ρ_r	kg/m^3	Plant life	t	years
Porosity	φ	%	Rejection temperature	T_r	°C
Rock specific heat	c_r	J/kg°C	Load factor	Lf	%
Temperature	T	°C	Power potential	P	MWe
Fluid density	ρ_f	kg/m^3			

2.3 Monte Carlo simulation

A Monte Carlo simulation is a simulation process based on generating model parameters that exhibit random behaviour. The name is taken from the city of Monte Carlo, which is famous for its gambling. Since it was first used to solve neutron diffusion problems in atomic bomb work at the Alamos Scientific Laboratory, Monte Carlo simulation has been widely applied to diverse problems such as complex physical and engineering problems. This is because the Monte Carlo simulation can be used for a large

number of random variables, various distribution types and nonlinear engineering models (Missouri University of Science and Technology, 2011).

According to Raychaudhuri (2008), to conduct a Monte Carlo simulation, several steps should be taken into account. First, the development of a deterministic model that closely resembles the real scenario by applying certain mathematical equations to the input variables and transform them into desired outputs. After the deterministic model is built, a good simulation should apply some risk components to the input variables. The risk parameters could be generated from historical data to determine the suitable probability distribution of the data, this procedure is called distribution fitting. In the Monte Carlo method, it is usual to assign some probability to build various versions of the model such as the most likely, the minimum value and the maximum value.

After the risk distribution is assigned to the input parameters, random numbers are generated from this distribution. One set of random numbers will be used in the deterministic model for each of the input parameters to produce one set of output values. This process is repeated with more sets of random numbers for each input distribution to generate more sets of output variables. This process is the core part of the Monte Carlo simulation. After the output values are collected, a statistical analysis is conducted for those values to provide the certainty and statistical confidence of the obtained values (Raychaudhuri, 2008).

Various styles of probability functions can be assigned to the volumetric model parameters. Most common are those of constant distribution, which means that all values between minimum and maximum estimates have the same likelihood. Another common probability function is that of triangular distribution where the minimum and maximum values are assigned less likelihood than a certain number, usually the mean value.

3. VOLUMETRIC CALCULATION

In this paper, two volumetric assessments will be discussed for two different geothermal areas at two different development stages, one in Corbetti in Ethiopia, which is in the early exploration stage and Rantau Dedap geothermal area in Indonesia, which is already delineated by exploration wells. By doing two different volumetric calculations, we should understand the difference between the assessment of probable reserves with Corbetti and proven reserves with Rantau Dedap area.

In the following section, the selection of each parameter for the volumetric calculations in both Corbetti and Rantau Dedap and also the result of the calculations, will be discussed. The programs, *Steamtab* (ChemicaLogic, 2018) and *Volumetric* (in-house ÍSOR - Iceland GeoSurvey software) are used here for these calculations.

3.1 Volumetric calculation of Corbetti

Corbetti geothermal area is located in the Mid-Ethiopian Rift (MER), about 200 km south of Addis Ababa. The area has been developed since the 1970s, currently by Reykjavik Geothermal. Corbetti is a promising area to be developed with earlier reserves estimations giving an estimate of over 1000 MW (Gíslason et al., 2015). The Gíslason paper mentions the estimated reserves but focuses more on the result of geoscience surveys without detailing the calculation itself. This paper will discuss the volumetric calculation in detail with information taken from the exploration surveys mentioned in Gíslason's paper.

Corbetti lies within an elliptical caldera of an area of 16×10 km^2, which is dominated with volcanological products of basaltic composition from its fissure eruptions with a post caldera infill of

rhyolitic rock such as obsidian lava and pumice (Gíslason et al., 2015). Traversing the caldera in the WSW-ESE direction is a volcanic belt with Mt. Uriji and Mt. Chebi as the local magma chambers. The belt contains craters, intersecting faults and together with the caldera rim these act as a controlling structure of geothermal surface manifestations.

The result of the resistivity survey was obtained by collecting both Transient Electromagnetic (TEM) and Magnetotelluric (MT) stations in about 150 locations. 1D modelling of these stations reveals a large low-resistivity anomaly, especially in the northern part of Corbetti caldera, which represents the clay cap of the geothermal reservoir (Figure 4). This clay-cap layer disappears south of Mt. Uriji, which is estimated to be a vertical resistivity boundary that is deep-rooted and extends down to more than 10 km depth. It is postulated that the vertical boundary is in the form of a transform fault within the rift zone (Gíslason et al., 2015).

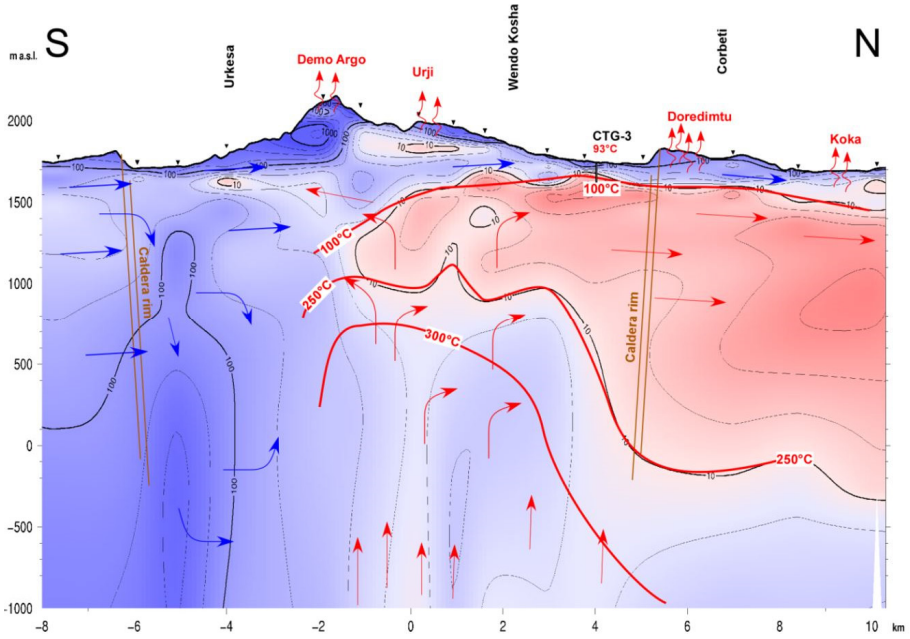

FIGURE 4: Conceptual model of Corbetti (Gíslason et al., 2015)

To make an estimation of the geothermal reserves, the *Volumetric* program which has been developed by ÍSOR – Iceland GeoSurvey will be used. The program basically works based on the Monte Carlo method and will provide the result of reserves estimation in probabilistic values.

One of the most important parameters for estimating geothermal reserves is the extent of the surface area of the reservoir. The area of the resistivity anomaly will be estimated based on the result of the resistivity survey, based on the area of high-resistivity under the low-resistivity anomaly (BOC, see Section 2.2.1). As the surface area is rather difficult to estimate, especially in this early exploration stage, three different values will be used in this work with 50 km^2 assigned as the minimum value, 75 km^2 is the most likely value and 100 km^2 is the maximum value.

The thickness of the reservoir is estimated from the bottom of the clay cap layer (BOC) extending to 3000 m depth (see Section 2.2.2). The estimate of the thickness also uses three different values with 1000, 1500 and 2000 m as the minimum, most likely and maximum values, respectively, in line with the cross-section in Figure 4.

The temperature of the reservoir used in the reserves estimation is based on steam geothermometers as there is no neutral chlorine hot spring in the Corbetti area. The atmospheric mixing of the steam is quite high within the caldera (80-98%) and lower in the caldera rim or outside (0-50%). That is why only the CO_2 geothermometer is used for the samples (Gíslason et al., 2015). The reservoir temperature used in

this paper also applied a triangular distribution, as with the reservoir surface area and thickness, with 259°C as the minimum temperature, 310°C as the most likely and 360°C as the maximum temperature. As the majority of rocks in Corbetti area are assumed of basaltic origin, for simplification, the volumetric calculation will only be based on basaltic rock properties. The *Volumetric* program provides the base rock type for the calculation. Hence it only needs the input of basalt rock type and the program will provide properties such as specific heat of the rock, which is 840 J/kg °C, and density of rock, which used constant distribution values with 2800 kg/m as the minimum value and 3000 kg/m^3 as maximum.

The properties of the reservoir fluid are derived from the reservoir temperature with the help of the *Steamtab* program developed by ISOR. For simplification and conservative prediction, a single-phase fluid with the most likely temperature of 310°C will be used for the estimation, which provides 690 kg/m^3 for density, 6084 J/kg°C for specific heat of the fluid and an enthalpy of 1402.2 kJ/kg, that will later be used for power plant efficiency estimation.

The porosity of the Corbetti geothermal reservoir is estimated by using existing data from the Aluto Langano geothermal area located near Corbetti with 10% porosity (WestJEC, 2016). The recoverable energy from the geothermal reservoir will be estimated from the relation between recoverable heat and the porosity as stated by Muffler and Cataldi (1978), which can be checked in Figure 2. The resulting recoverable heat, which will be used in the calculations, is 0.25 in accordance to a porosity value of 0.1.

The rejection temperature for the power plant is assumed to be 180°C, which is the usual temperature for single-flash conventional power plants according to Sarmiento et al. (2013). The efficiency of the power plant will be estimated using Equation 3 developed by Moon and Zarrouk (2012) based on a collection of geothermal power plants efficiency around the world and their respective reservoir temperature.

$$\eta = 8.7007 \ln(h) - 52.335 \quad (3)$$

With an enthalpy value of 1404.2 kJ/kg from the *Steamtab* program, the efficiency obtained from the above equation is 10.7%. According to Sarmiento et al. (2013), a good geothermal power plant will have a load factor of 90-97%, so in this paper a load factor of 95% is chosen for the volumetric calculation input. Data on the 25 years of geothermal utilization in Ethiopia will also be put into the *Volumetric* program.

All the parameters for the *Volumetric* program inputs are shown in Table 2. It should be noted that some of the parameters contain three different values, minimum, most likely and maximum such as the surface area, reservoir thickness and reservoir temperature, while other values are fixed values, such as porosity,

TABLE 2: Input parameters for the Corbetti reserves calculation with the *Volumetric* program

Input variables	Symbol	Units	Min.	Most likely	Max.	Type
Surface area	A	km^2	50	75	100	Triangular
Thickness	h	m	1000	1500	2000	Triangular
Rock density	ρ_r	kg/m^3	2800	2900	3000	Constant distribution
Porosity	Φ	%		10		Fixed value
Rock specific heat	c_r	J/kg°C		840		Fixed value
Temperature	T	°C	259	310	360	Triangular
Fluid density	ρ_f	kg/m^3		f (T)*		
Fluid specific heat	c_f	J/kg°C		f (T)*		
Recovery factor	R	%		25		Fixed value
Conversion efficiency	η	%		10.7		Fixed value
Plant life	t	years		25		Fixed value
Rejection temperature	T_r	°C		180		Fixed value
Load factor	Lf	%		95		Fixed value

*f (T) means the value is a function of temperature

recoverable energy and fluid and rock properties. The reason behind this is to simplify the calculation by only giving a distribution to the most important parameters and also to the parameters that are quite hard to determine exactly.

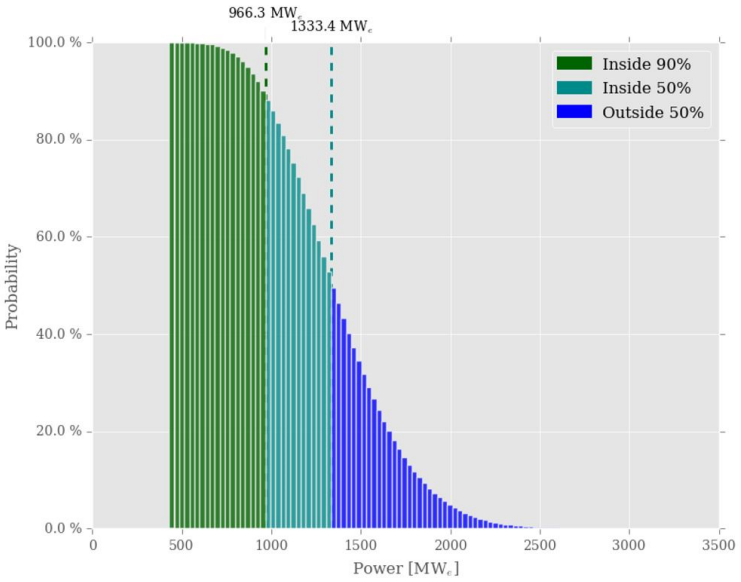

FIGURE 5: Result of reserve estimation in Corbetti calculated with the *Volumetric* program

The resulting calculation from the *Volumetric* program is shown in an output cumulative histogram of megawatts of electricity in Figure 5. The P90, or 90% probability, has a value of 970 MWe and P50, or 50% probability, has a value of 1330 MWe. These are the most common prediction values in reserves estimation. Aside from giving almost the same result as the previous estimation by Gíslason et al. (2015), which is 1000 MWe, the results in this paper also provide more detailed values because the previous paper only used power density for reservoir assessment.

3.2 Volumetric calculation of Rantau Dedap

Rantau Dedap is a geothermal area located in South Sumatera province, Sumatera, Indonesia. Currently under development by PT. Supreme Energy Rantau Dedap (SERD), the exploration study of Rantau Dedap started in 2008 with geological, geochemistry and geophysical studies. Rantau Dedap geothermal area is associated with two parallel faults, of which one is the Great Sumatra Fault (GSF) and the other is a regional fault system with a NW-SE direction. Aside from the NW-SE faults, there are faults in the NE-SW direction and the N-S direction that together control the distribution of geothermal surface manifestations, such as fumaroles and hot springs. A circular feature is also found in the form of Semendo caldera, which is translated as the boundary of the geothermal system (PT. Supreme Energy Rantau Dedap, 2015).

Geological features in Rantau Dedap are mostly dominated by volcanic breccia, basaltic-andesite lava and pyroclastic tuff. From volcano stratigraphy mapping, there are at least nine volcanic products in which the Bukit Besar volcanic product is estimated as the source of the reservoir rock. The Bukit Besar volcanic product shows a radial morphology of circular fault features that indicates a former caldera structure.

The geophysical survey was conducted in 2008 with MT measurements at 90 stations and a 3D model generated from the data. The analysis of the data shows a low-resistivity body extending from Bukit Mutung and Bukit Balai in the north to Anak Gunung and Bukit Besar in the south. The low-resistivity body, which is translated as a clay cap layer, shows a dome-like structure under Bukit Besar and Air Kelat-Indikat Tengah, which indicates the upflow zones. With the assumption that the BOC is the same as the top of reservoir (TOR), the resistivity survey resulted in an estimation of TOR to be 500-1000 m a.s.l.

After all geoscience surveys were completed, exploration drilling in Rantau Dedap was started in February 2014 and ended in April 2015. Six directional exploration wells (RD-B1, RD-B2, RD-C1, RD-I1, RD-I2 and RD-C2 in chronological order) were drilled to the range of 2200-2700 m depth (PT. Supreme Energy Rantau Dedap, 2015). Comprehensive well testing surveys were conducted after

drilling completion such as pressure and temperature (PT) logging, multi-stage injection tests, production tests and interference tests to better understand the reservoir parameters (Humaedi et al., 2016).

From the interpretation of the well testing, especially the PT logging, a conceptual model was built in the SW-NE direction as shown in Figure 6. From the conceptual model, we can see that the upflow zone is southwest of well I2 where 300°C waters travel in diagonal plume until at 800-1200 m a.s.l. where the temperature drops to 230°C and then moves in a horizontal direction towards the northeast where the temperature gradually declines to 220-210°C. The deep recharge from the northeast direction is interpreted from the low pressure in deep well I2 and temperature reversal in some of the wells (Bacquet et al., 2016).

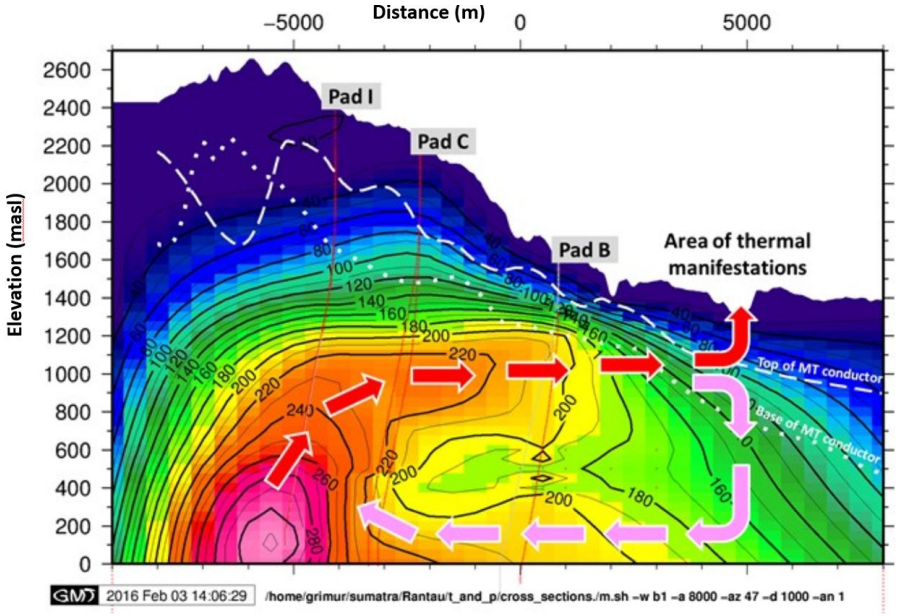

FIGURE 6: Conceptual model of Rantau Dedap in the SW-NE direction (Bacquet et al., 2016)

The determination of parameters as the input for the reserves calculation for the Rantau Dedap area is rather different than the one used in Corbetti. With the improvement of the understanding of the geothermal reservoir supported by exploration well drilling and well testing, the parameters used are significantly more dependable. For example, when deciding the surface area of the reservoir, estimation using the resistivity survey result is not used. Instead, the extent of the surface area is decided based on a model of temperature vs. surface area for different depths developed by a Supreme Energy team that was derived from temperature well logging data (Björnsson and Novianto, 2015).

The input of surface area and temperature in the *Volumetric* program will also use three different values based on the model for 200 m a.s.l. or the bottom hole elevation of most of the wells (see Table 2 in Björnsson and Novianto, 2015). A temperature of 230°C will be used as the minimum value which corresponds to 17.1 km^2 in the model, 250°C will be used as the most likely value which corresponds to 11.3 km^2 and a maximum value of 290°C will be used which corresponds to 3.2 km^2. So, the surface area will use 3.2, 11.3 and 17.1 km^2, while the reservoir temperature will use 230, 250 and 290°C as the minimum, most likely and maximum values, respectively.

The thickness of the reservoir is predicted from the results of temperature and pressure loggings as seen in Figure 7. From the graph, one can see that there are two different main heat transfers that happen in the reservoir. From the surface to the depth of about 1200 m a.s.l., conduction is dominating the heat transfer, while from 1200 m a.s.l. to bottom of the wells, convection dominates the heat transfer as indicated by the isothermal line in the graph. The thickness of the reservoir that will be used in the program is 1200 m for the minimum, 1300 m for the most likely and 1400 m for the maximum value.

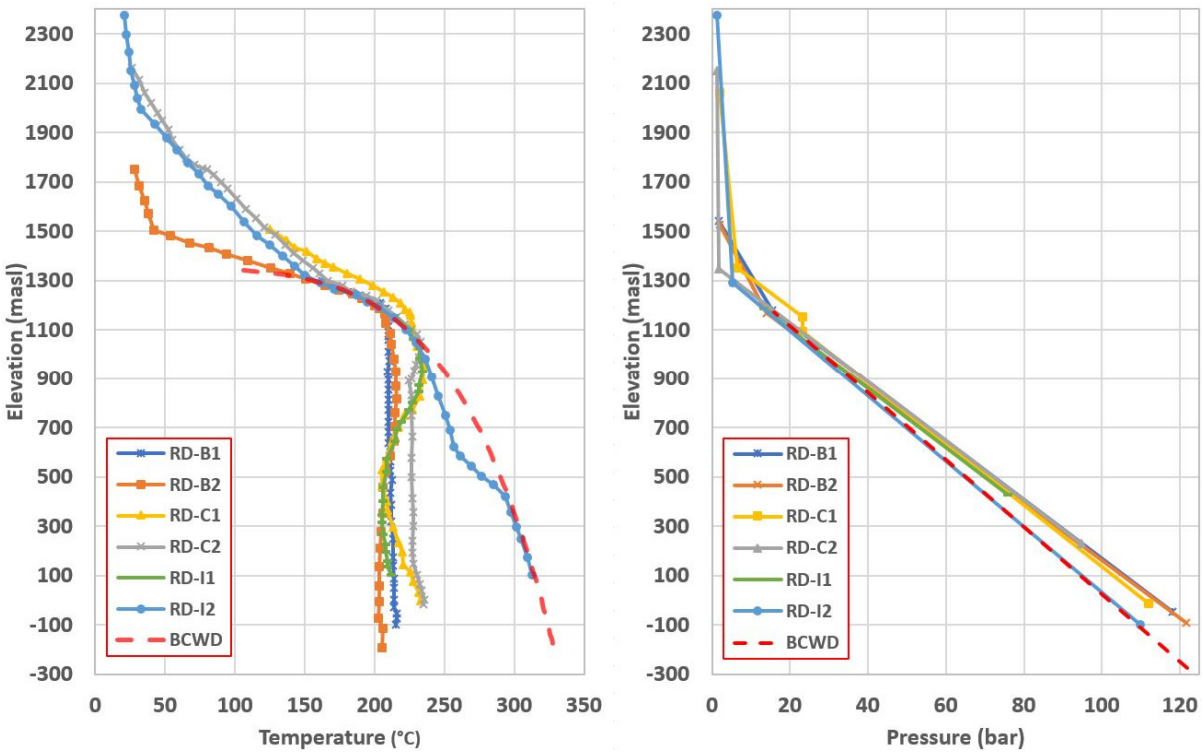

FIGURE 7: Interpreted initial temperature and pressure of Rantau Dedap (modified from Bacquet et al., 2016)

The properties of the reservoir are divided into two categories, which are the rock properties and the fluid properties. For the input of rock properties, the *Volumetric* program only needs the input of the rock types and it will provide the parameters. As the majority rock type in Rantau Dedap is andesitic, the andesite type is used. The program provides the specific heat of the rock, which is 1000 J/kg°C, and the density of the rock, which uses constant distribution values with 2500 kg/m as the minimum value and 2800 kg/m^3 as the maximum value.

The estimation of the reservoir temperature in Rantau Dedap is also more dependable than for Corbetti because it is based on downhole data. The input is based on the 138th day of the discharge test of well I2, which resulted in a dryness of 31% and enthalpy of 1407 kJ/kg. The value of dryness and temperature of 250°C are put into *Steamtab* program, which gives 557 kg/m^3 for the density and 4606 J/kg°C for the specific heat of the fluid. The obtained enthalpy is used in Equation number 3 which results in an efficiency of 10.7%.

The porosity is assumed to be 10% as usual for geothermal areas in a volcanic systems, which also corresponds to a recoverable heat of 25% according to Muffler and Cataldi (1978). The rejection temperature for a single-flash conventional power plant is 180°C. The load factor of the power plant will be 95%, while a utilization period of 30 years will be used in accordance with geothermal policy in Indonesia.

All the parameters above are listed in Table 3 to be inputted into the *Volumetric* program.

The result of the estimation as shown in Figure 8 provide a P90 of 49.3 MWe and P50 of 82 MW which is significantly lower than the 220 MWe of reserves estimation stated in the Geothermal Working Area tender document of Rantau Dedap. This can be the case when the estimation is done in more developed conditions. This usually leads to the estimation becoming smaller as more information is obtained. This is mainly because the estimation of the surface area in earlier development is usually based on resistivity

surveys, which can provide a too optimistic result. In particular if the reservoir outflow zone has been cooling down over geological time scales as appears to be the case in Rantau Dedap. In such situations, TOR is not the same as BOC resulting in an overestimation of the reservoir area.

TABLE 3: Input parameters for Rantau Dedap reserves calculation with *Volumetric* program

Input variables	Symbol	Units	Min	Most likely	Max	Type
Surface area	A	km^2	3.2	11.3	17.1	Triangular
Thickness	h	m	1200	1300	1400	Triangular
Rock density	ρ_r	kg/m^3	230	250	290	Triangular
Porosity	Φ	%		10		Fixed value
Rock specific heat	c_r	J/kg°C		1000		Fixed value
Temperature	T	°C	230	250	290	Triangular
Fluid density	ρ_f	kg/m^3		f (T)		
Fluid specific heat	c_f	J/kg°C		f (T)		
Recovery factor	R	%		25		Fixed value
Conversion efficiency	η	%		10.7		Fixed value
Plant life	t	years		30		Fixed value
Rejection temperature	T_r	°C		180		Fixed value
Load factor	Lf	%		95		Fixed value

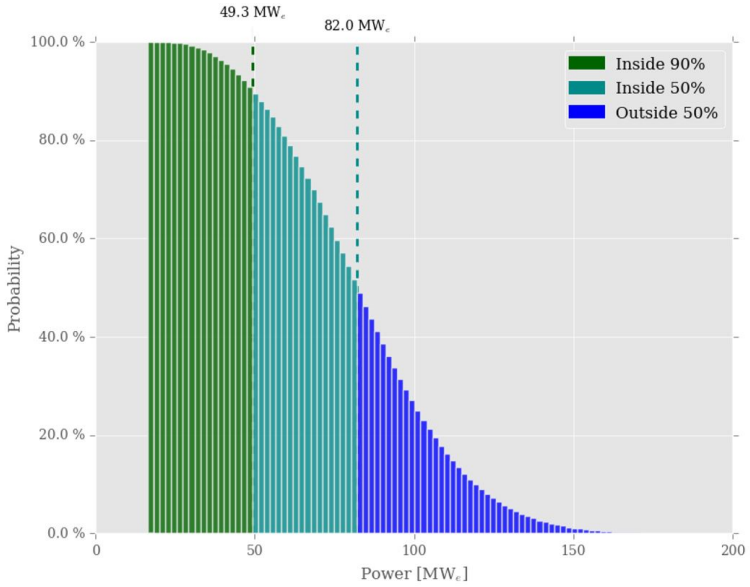

FIGURE 8: Result of the reserve estimation in Rantau Dedap in single-flash system with the *Volumetric* program

The geothermal energy in Rantau Dedap could be utilized more in the form of bottoming the rejected fluid from the separator, as the rejected fluid with 180°C temperature still contains a lot of energy. The energy can be utilized by applying a second low-pressure turbine or a binary system. Here, an attempt is made to estimate the additional power generation with a binary system. Almost all of the parameters used in the second calculation for a binary system in Rantau Dedap are the same as for the single-flash calculation. The difference is the inlet temperature that will be 180°C and the rejection temperature of binary system that will be 120°C.

The properties of the fluid will be estimated using the *Steamtab* program which provides 886 kg/m^3 for the fluid density and 4404 J/kg°C for the specific heat of fluid. The efficiency of a binary power plant is obtained using Equation 4 (Moon and Zarrouk, 2012):

$$\eta \text{ binary} = 6.9681 \ln(\text{Tin}) - 29.713 \quad (4)$$

Using the above equation, the binary power plant efficiency is 6.5%. The value together with the fluid properties and rejection temperature are put into the *Volumetric* program and provides the result as shown in Figure 9. The result shows a P90 of 25.9 MWe and P50 of 42.3 MWe, which could be extracted additionally to the condensing steam approach in Rantau Dedap. Further study should be done to estimate the feasibility of applying a bottoming system in general, as it will require more investment in the project. A double-flash and two-inlet turbine design should also be considered as it allows a more efficient conversion of the geothermal heat to power.

4. WELL LOGGING ANALYSIS

In this section, analysis of logging in a geothermal well will be discussed. The well that will be used is well SV-26 in Svartsengi in the Reykjanes peninsula, SW-Iceland. Svartsengi is a geothermal area that has been in development since the early 1970s. The first well was drilled in 1971, and the first geothermal exploitation started in 1976 (Björnsson and Steingrímsson, 1992). The power plant is currently producing 76 MWe of electricity and some additional 300 MW of heat (Georgsson, 2017).

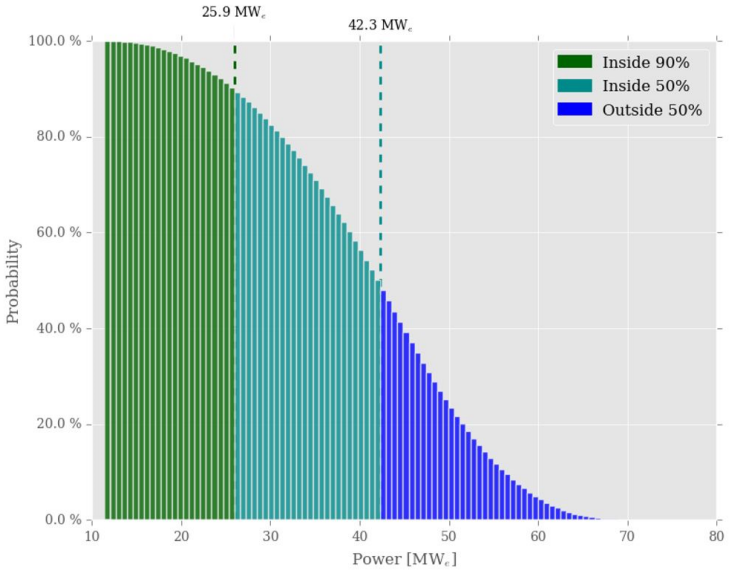

FIGURE 9: Result of the reserve estimation in Rantau Dedap for a binary system with the *Volumetric* program

The area is located in an active rift zone, which is the extension of the Mid-Atlantic ridge. It is situated in a basaltic rich surface with a sequence of lava flows and hyaloclastites underneath. The reservoir was initially in a liquid-dominated phase with temperatures between 230 and 240°C and salinity corresponding to 2/3 that of seawater. With continuous production, there has been an expansion of a shallow two-phase zone due to pressure drawdown of the system (Björnsson and Steingrímsson, 1992).

Well SV-26 is located southeast of the Svartsengi power plant. It was drilled in a directional inclination to reach 2537 m measured depth (MD). The drilling was finished on March 1st, 2016 (Weisenberger et al., 2016). All the well design parameters and measurements, which are in m MD, were processed with the ICEBOX program to be converted to true vertical depth (TVD) as shown in Figure 10 (Arason et al., 2004).

The well was then continuously tested and logged through various kinds of tests to obtain the reservoir parameters during and after the well completion. The temperature loggings were conducted during and after the drilling. One of their main objectives was to predict the locations of the feedzones in the well. Aside from the temperature loggings, other loggings were also conducted such as pressure, XY-caliper, dual neutron, gamma resistivity and cement bond log (CBL) loggings.

Here, the focus is on the temperature and pressure loggings. These data are plotted against TVD and compared to well design to better understand the properties of the well and the reservoir as shown in Figure 10. The temperature and pressure loggings in the well were conducted during different states of the well, such as during injection, warming up period, static condition and also during discharge condition. The measurement points are also tightly spaced with generally 0.5 m distance between measurement points to provide a more accurate interpretation in the logging analysis.

From the analysis of the temperature and pressure logging, as shown in Figure 10, valuable information about the well and the reservoir is obtained. For example, from the temperature logging in the injection and static well, a prediction of the feed points of the reservoir in the well could be made. The feed points can be inferred by the injection temperature runs such as the ones dated on February 25th and 27th and also March 2nd, 2016. When comparing the loggings dated February 25th and 27th, one can see the difference where the later loggings show a sudden temperature changes at 1225 m TVD, while the previous loggings show just slight changes of slope temperature vs. depth at that depth.

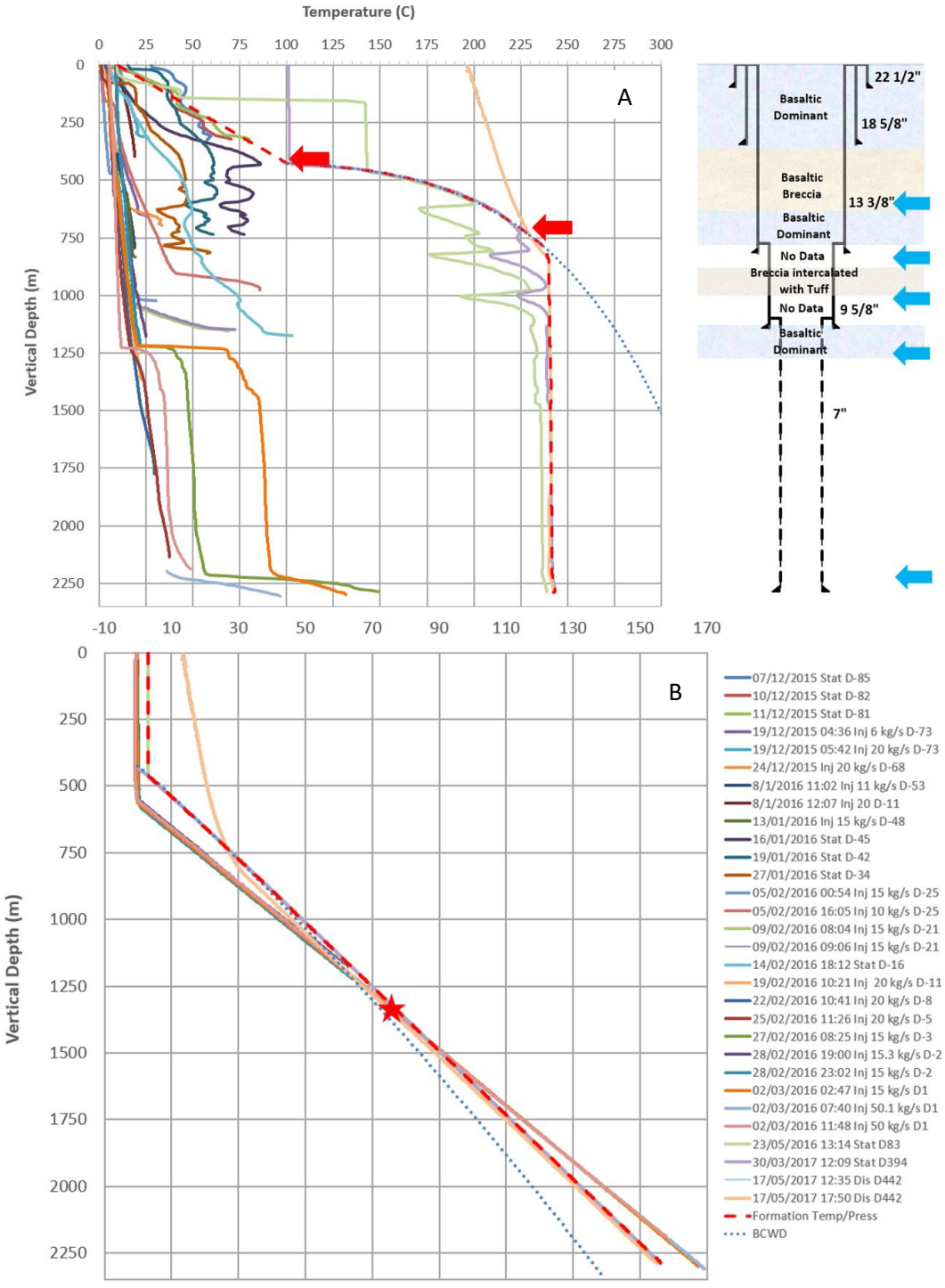

FIGURE 10: Well SV-26, a) Temperature logging and well design; and b) Pressure logging analysis

Analysis of both of the loggings actually shows that there is a feedzone at 1225 m TVD, the difference is the logging on February 25th was conducted during injection of 20 kg/s of cold water while the later logging was conducted during injection of 15 kg/s of cold water. The differential flow of fluid injected causes differential well pressure. In the logging on February 25th, the well pressure in 1225 m TVD is higher than that of the reservoir, which is why the feedzone acts as an outflow in that condition with partial loss of the injected fluid. The logging on February 27th shows that due to 15 kg/s of injection, the well pressure in the 1225 m TVD feedzones is lower than the reservoir which is why hot reservoir fluid

flows into the well, causing sudden changes in temperature. This logging also shows a total loss of circulation (TLC) zone at 2200 m TVD where all of the injected fluid is flowing out to the reservoir.

The feed points can also be inferred from static well loggings where there is a part in the logs where the temperature is much lower than its surrounding temperature, as shown from loggings dated May 23rd, 2016 and March 30th, 2017. From the loggings, some feed points could be located at 625, 825 and 1000 m TVD that are now behind the cemented casing. The lower temperature of those depths is because they are the feedzones that have been cooled by the injection and at that time contain cold water and drilling fluid, while the higher temperature is for the impermeable ones, which have been cooled conductively.

From the static temperature logging conducted on May 23rd, 2016 and March 30th, 2017, and also the discharge logging dated May 17th, 2017, one can predict the reservoir fluid condition when entering the well. From the graph, it is predicted that the fluid entering the well is in a liquid-phase condition and has a temperature of 240°C. Interzonal flow happens in the well between the depth of 1200 m TVD where the casing ends down to the bottom of the well. It is categorized by an isothermal line in the well, which heats up more quickly than the other parts. As the shallower part of well has lower pressure than the deeper part, the reservoir fluid in the well begins to boil around 700 m TVD. This is indicated where the graph starts to coincide with the boiling point curve with depth (BCWD). The difference between loggings dated May 23rd, 2016 and March 30th, 2017 is that in the previous log, the upper part of the well is still full of cold gas, while the later log, that was conducted almost a year later, shows that the upper part of the well is full of saturated steam with a temperature of 100°C.

The boiling in the well prediction is also supported by the pressure logging results where all the pressure loggings show higher measured pressure than pressure in the BCWD. Other information that can be obtained from the pressure logging was the location of static water table at 425 m TVD. From the pressure analysis, we can also see the location of the pivot point of the well at 1350 m TVD. The pivot point is a certain depth in the well where the pressure does not change along the warm up surveys. The pressure at the pivot point is the best indication of the real pressure of the reservoir, which is 77 bar-g. When the result is crosschecked with the temperature loggings and the well design, the pivot point is located between two major feedzones at 1225 and 2200 m TVD, which usually happens in wells with more than one major feedzone (Grant et al., 1982).

One of the reservoir properties that is hard to pinpoint is the formation/reservoir temperature, even after drilling and well logging. According to Kutasov and Eppelbaum (2005), people usually determine the formation temperature based on the bottomhole temperature in the well, but this method does not necessarily provide the best estimation as drilling and injection alter the reservoir temperature in the well. The temperature of the fluid in the well is furthermore affected by the duration of drilling fluid circulation, the difference between the reservoir and drilling fluid temperature, well radius, thermal diffusivity of the reservoir and the drilling technology (Kutasov and Eppelbaum, 2005).

One of the methods that are used to estimate the formation temperature is using the Horner plot that has been widely used in petroleum engineering since the early 1950s. The Horner method assumes that the well is cooled for a time (t_p), and the temperature is measured several times (Δt) after the circulation stopped. The formation temperature is estimated by plotting the data on a Horner plot and extrapolating it to $\Delta t = \infty$, or $(tp + \Delta t)/ \Delta t = 1$. The Horner plot is based on the heat conduction equation:

$$(\rho C)\frac{\delta T}{\delta t} = K\nabla^2 T \tag{5}$$

This method only governs the cooling and warming when conduction is the dominant mechanism in a well and therefore the method is less valuable when applied to a zone of fluid loss or another permeable zone (Grant et al., 1982).

The formation temperature estimation in this paper uses the *Berghiti* program (Arason et al., 2004), developed by ÍSOR that works based on the Horner method (Marteinsson, 2017). In Figure 10a, one can

see that the formation temperature is around 240°C where the resulted value from *Berghiti* is almost the same as the temperature logging conducted in the well (March 30th and May 17th 2017). This is because when the loggings were conducted, the well had already heated up for over a year, and hence is already in equilibrium with the formation temperature of the reservoir. When applying the Horner method to the upper part of the well, the resulting temperature gives a rather implausible result, which is why the formation temperature was predicted manually.

5. INJECTION AND PRODUCTION TESTS

Along with temperature and pressure logging interpretation, it is of interest to analyse the injection and production tests that were conducted on well SV-26. The purpose of conducting such tests, is mainly to estimate the permeability of the well through injectivity or productivity indices. Before conducting multistage injection or production tests, first of all the location of the feedzones in the well should be estimated (Haraldsdóttir, 2017), as the injectivity, productivity or effective permeability values are bound to a certain feedzone. This is why prediction of major feedzones as conducted in the previous section is of importance.

The value of reservoir flow in or out of the well does not necessarily imply a small or large value of permeability. The permeability could be estimated by the change of pressure in the intended measured feedzone when different injection rates are applied to the system. As mentioned before, placing measuring devices in the exact location of the feedzone is important as placing the pressure gauge in the wrong level of the well may cause irregular or oscillatory results in the data analysis (Grant et al., 1982).

In well SV-26, two multistage injection tests were conducted after the drilling was completed. The first was conducted on February 28th, 2016 and the second one two days later, on 2nd March 2016. A multistage production test was then conducted more than a year later, on May 17th, 2017.

5.1 First multistage injection test

The first multistage injection test was conducted on February 28th, 2016 or two days before the drilling finished as the test was conducted before the 7'' slotted liner was installed in the well (Weisenberger et al., 2016). The pressure measurement tool was placed at 1225 m TVD in the shallower feedzone of the two major feedzones found in the well as shown in Figure 10. An injection rate of 15.3 kg/s was maintained for some time in the well and then the injection rate was increased to 50 kg/s and then the injection was decreased again to 15 kg/s. The measured pressure was plotted against time as shown in Figure 11.

From the plot, one can see that some of the collected data are not uniform, which is why some measurement points should be modified or even excluded when doing hydrological modelling. As an example, in the early increase of injection, the measurement part that is used is starting from 0.4 hours instead of at 0.

The plotted data is then used as a source to estimate the injectivity index of the 1225 m TVD feedzone. The initial injection rate of 15.3 kg/s corresponds to a pressure of 64.4 bar, while the first stage injection rate of 50 kg/s corresponds to a pressure of 66.3 bar and second stage injection rate of 15 kg/s corresponds to a pressure of 63.7 bar. It should be noted that the pressure above is pressure at the end of the step where it is assumed it has reached stability. The three-stage multistage injection test is then plotted in a pressure versus injection rate graph as shown in Figure 12.

After the data were plotted, a linear trendline was made in the graph. The injectivity index is the ratio between the change of injection rate into the well, which causes a certain change in well pressure or can be generated from the slope of the resulted trendline which is 14.3 kg/s/bar.

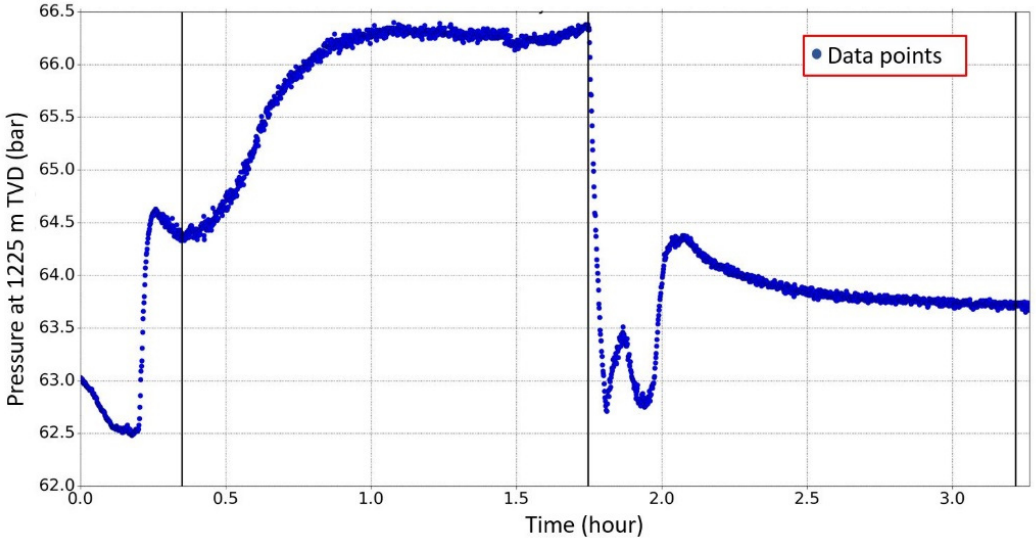

FIGURE 11: The first multistage injection test of well SV-26 before running the liner (February 28th, 2016)

The multi-stage injection test is then modelled with the *Welltester* program developed by ÍSOR to obtain reservoir properties such as transmissivity, storativity, skin factor and other parameters. Transmissivity is the ability of the reservoir to transmit fluid while storativity is the ability of the reservoir to gain or release a certain volume of fluid per unit pressure changes per unit area (Grant and Bixley, 2011). Wellbore storage is the wellbore capacity to store fluid. The skin value is representing a reservoir zone close to the well where there may exist a different value of permeability, usually from side effect of drilling such as stimulation or formation damage from cuttings or drilling mud (Grant et al., 1982). The well is in a good condition if the skin value is negative, which means the skin zone permeability is higher than those of the reservoir. Vice versa a positive skin value means there is some damage in the well that reduces its permeability (Horne, 1995).

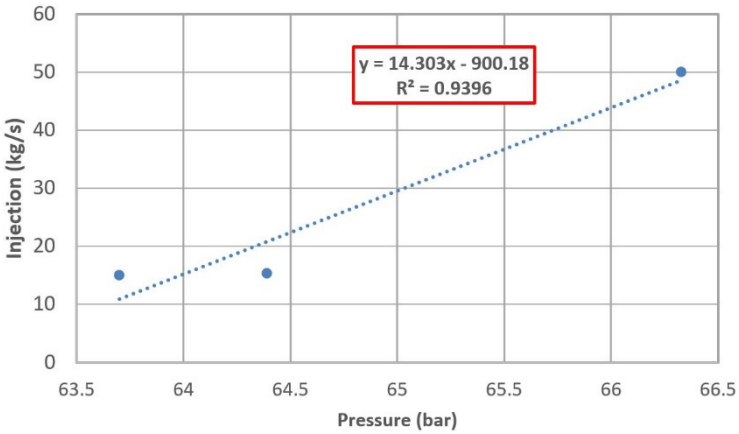

FIGURE 12: Injectivity index estimation of well SV-26 based on the first multistage injection test (February 28th, 2016)

When doing modelling for the injectivity test, some measurement points, usually in the beginning or ending of each step have to be modified or omitted as they show instability and will tamper the result of the modelling. Examples of measurement points omitted during the *Welltester* modelling for multistage injectivity text are shown in Figures 13 and 14.

For the model calibration, several initial model parameters are assumed and will be inverted by *Welltester*. Other parameters such as wellbore radius and reservoir temperature could refer to the previous logging result. Other parameters that have to be assumed are porosity, dynamic viscosity, total compressibility of the reservoir, etc. The *Welltester* program provides many kinds of conditions for the modelling but in this paper a homogenous porosity of the reservoir, boundary condition which refers to

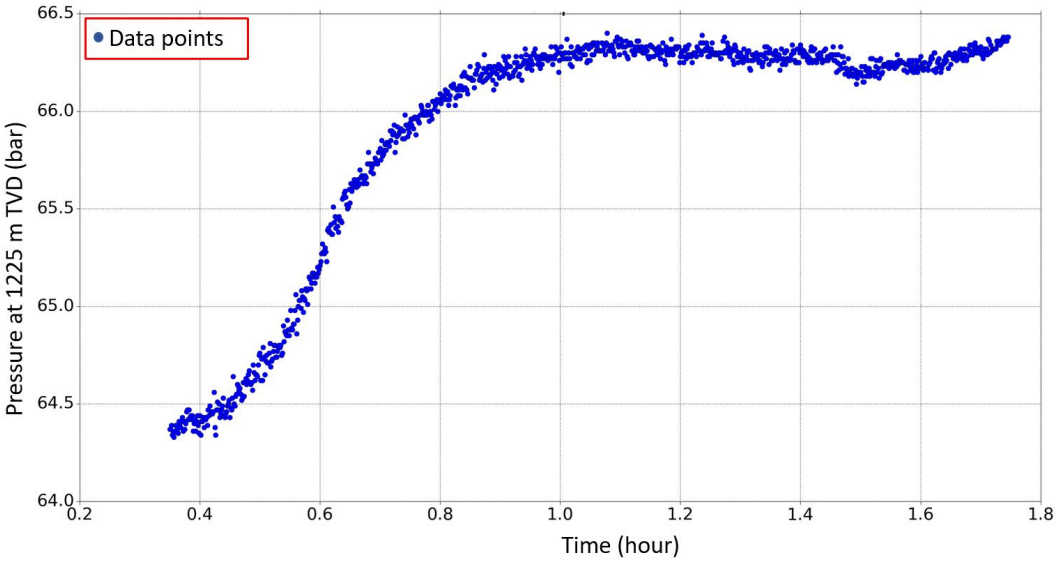

FIGURE 13: The first step of the first multistage injection test (February 28th, 2016)

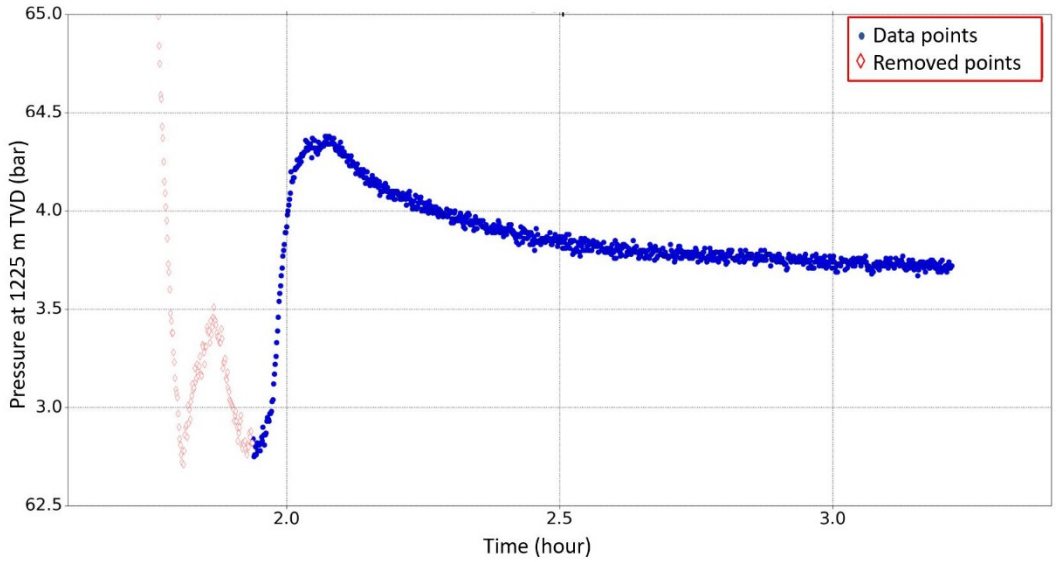

FIGURE 14: The second step of the first multistage injection test (February 28th, 2016)

a constant pressure, constant skin value for the well and also constant wellbore storage would be assumed as the reservoir conditions for the modelling.

Figure 15 and 16 show the result of the modelling which uses a logarithmic scale for the pressure changes and the timescale together with the derivative for the pressure response multiplied by time difference since the beginning of the steps. Modelling using a derivative plot is commonly used to determine the best-fitted model for certain measured data. Figures 15 and 16 show the modelling of the first step and the second step, respectively. The reservoir properties obtained from the modelling will be discussed in a later part of this paper.

5.2 Second multistage injection test

The second multistage injection test was conducted on March 2nd, 2016 or one day after the drilling was completed. The pressure tool was placed at 2200 m TVD close to the bottom of the well where TLC happens (see Figure 10). The well was initially injected with 15 kg/s water, which was maintained for

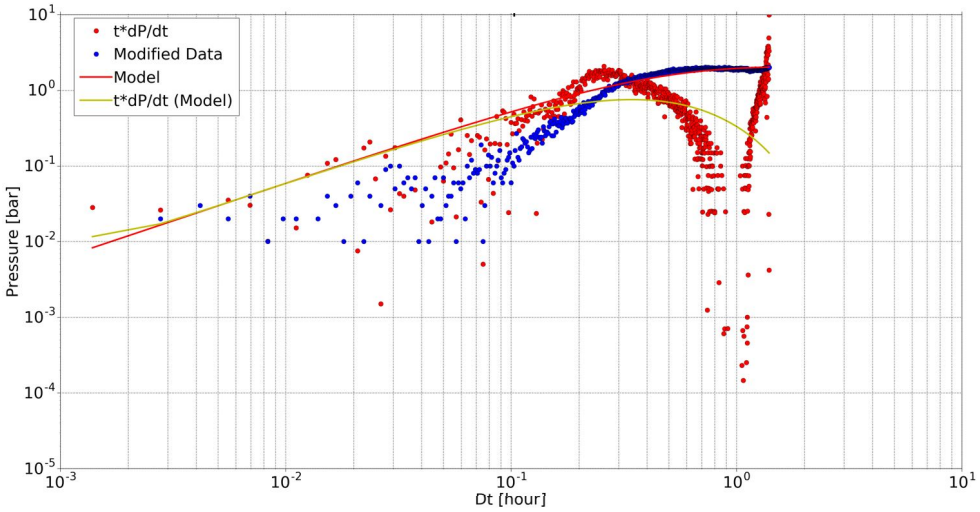

FIGURE 15: The modelling result of the first step of the first multistage injection test (February 28th, 2016)

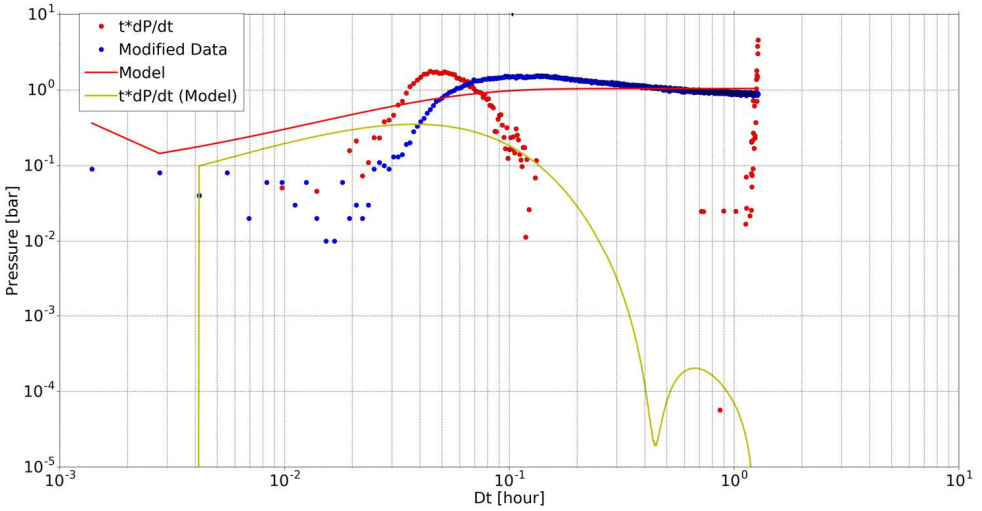

FIGURE 16: The modelling result of the second step of the first multistage injection test (February 28th, 2016)

some time, corresponding to a well pressure of 157.0 bar. Then the well was injected with water of flow rate 50 kg/s, which corresponded to a pressure of 158.4 bar. The injection was decreased again to 15 kg/s, which corresponded to a well pressure of 155.1 bar and lastly, the injection was increased again to 50 kg/s, which corresponds to a pressure of 158.3 bar. As with the first injection test, the pressure here is the end of step pressure when the pressure has already stabilized. All the pressure measurements were plotted against time as shown in Figure 17.

The stabilized pressure of each step was plotted against their corresponding injection rate, as shown in Figure 18. A linear trendline was then made which generated a linear equation of y = 11.38x – 1756.4 which means that the injectivity index for the second multistage test was 11.4 kg/s/bar.

The second multistage injection test was also modelled with the *Welltester* program to obtain the reservoir properties. First of all, the same properties as applied in the first multistage injection test should be assumed as an initial value for the program. This second test should also use the same type of modelling as the first one with homogeneous porosity, constant pressure boundary, constant wellbore storage and constant skin value. The modelling result is shown with logarithmic pressure and timescale with the data, and modelling results based on measured points and their derivative with Figure 19

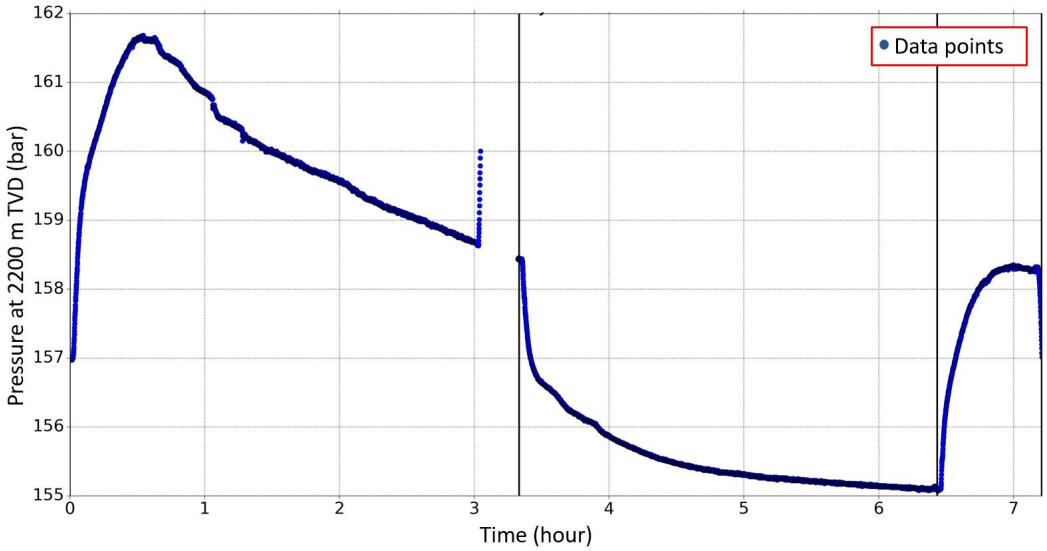

FIGURE 17: The second multistage injection test (March 2nd, 2016)

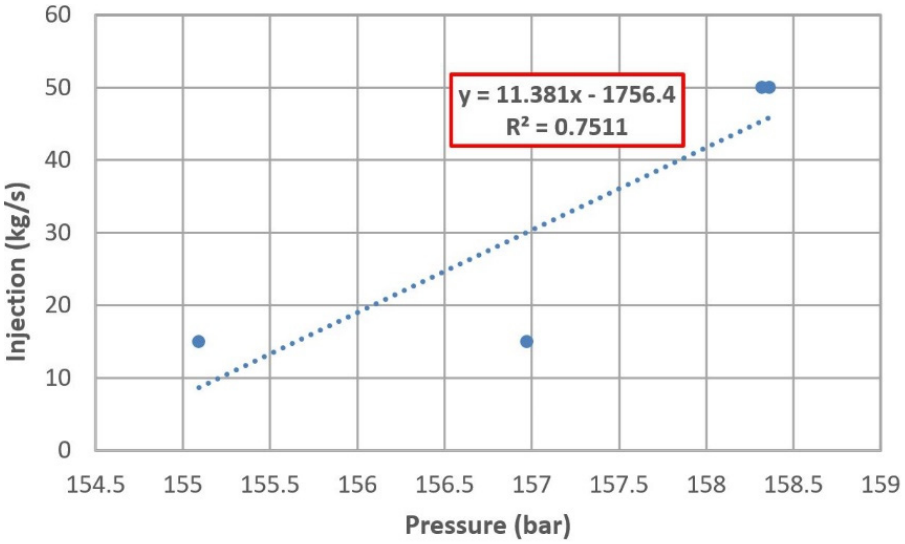

FIGURE 18: Injectivity index estimation of well SV-26 based on the second multistage injection test (March 2nd, 2016)

showing the first step, Figure 20 shows the second step and Figure 21 shows the third step. The parameters obtained are shown in Table 4.

5.3 Multistage production test

The multistage production/discharge test basically has the same characteristics as an injection test, one difference is the direction of the flow. While the injection test is injecting a certain mass to the geothermal system, production test discharges a certain mass of the reservoir fluid out of the system. The method of measuring the productivity index is also the same as measuring the injectivity index as has been discussed before. The production test in well SV-26 was conducted on May 17th, 2017, or 422 days after drilling was completed (Thorgilsson et al., 2017). The long interval between drilling completion and the production test was to give the well time to heat up so it could have enough energy to self-discharge, after being cooled during drilling and injection tests.

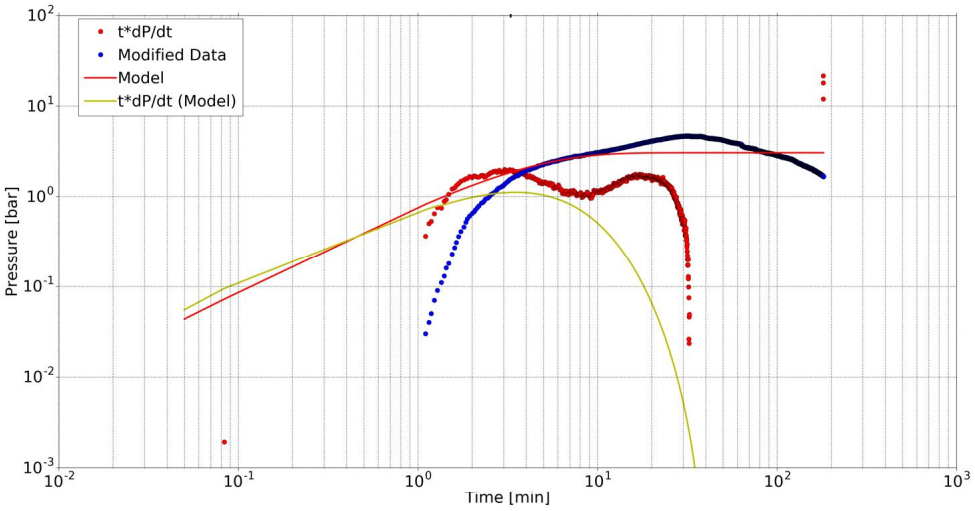

FIGURE 19: The modelling result of the first step of the second multistage injection test (March 2nd, 2016)

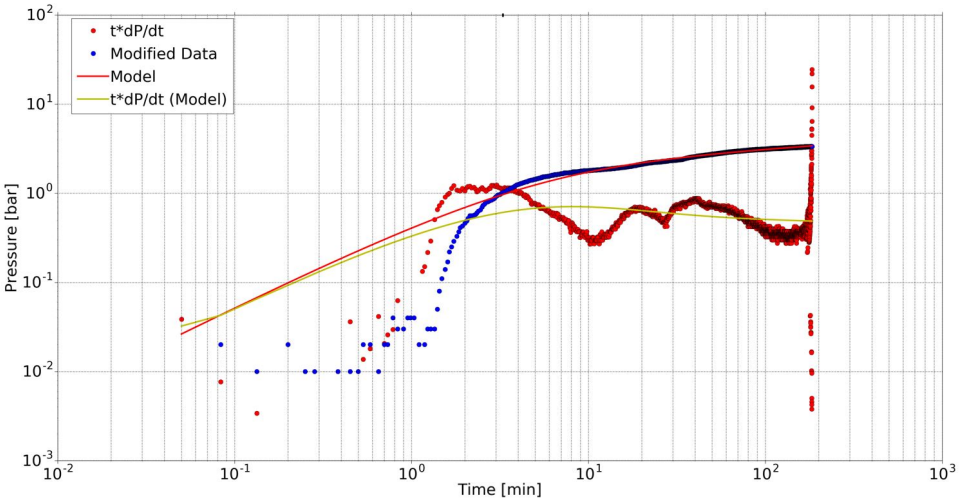

FIGURE 20: The modelling result of the second step of the second multistage injection test (March 2nd, 2016)

TABLE 4: Reservoir parameters of well SV-26, Svartsengi, based on well testing analysis with homogenous model of *Welltester*

Parameter	Injection test 1 without liner		Injection test 2 with liner			Production test 1 with liner		
	Step 1	Step 2	Step 1	Step 2	Step 3	Step 1	Step 2	Step 3
Transmissivity (m^3/ Pa s)	1.32×10^{-7}	1.88×10^{-7}	9.76×10^{-8}	6.02×10^{-8}	1.02×10^{-8}	4.34×10^{-7}	2.18×10^{-7}	1.61×10^{-7}
Storativity (m/Pa)	5.96×10^{-8}	1.87×10^{-10}	8.71×10^{-10}	7.00×10^{-8}	7.66×10^{-8}	7.06×10^{-7}	1.38×10^{-6}	1.76×10^{-7}
Radius of investigation (m)	13.5	10	84.39	258.92	28.69	131.66	25.55	10.00
Skin factor	0.50	-7.65	-0.91	-3.11	-4.59	4.64	-0.49	-0.70
Wellbore storage (m^3/ Pa)	2.09×10^{-4}	6.94×10^{-6}	2.39×10^{-5}	3.77×10^{-5}	1.61×10^{-5}	3.27×10^{-5}	2.63×10^{-5}	2.76×10^{-5}
Reservoir thick.(m)	403	1.26	6.41	515.30	564.18	5156.55	10064.43	1284.25
Injectivity index (l/(s bar))	17.1	33.6	11.47	10.31	10.75			
Productivity index (l/(s bar))						25.31	29.71	29.39
Effective permeability (m^2)	3.67×10^{-14}	1.67×10^{-11}	1.74×10^{-12}	1.34×10^{-14}	2.07×10^{-15}	9.61×10^{-15}	2.47×10^{-15}	1.43×10^{-14}

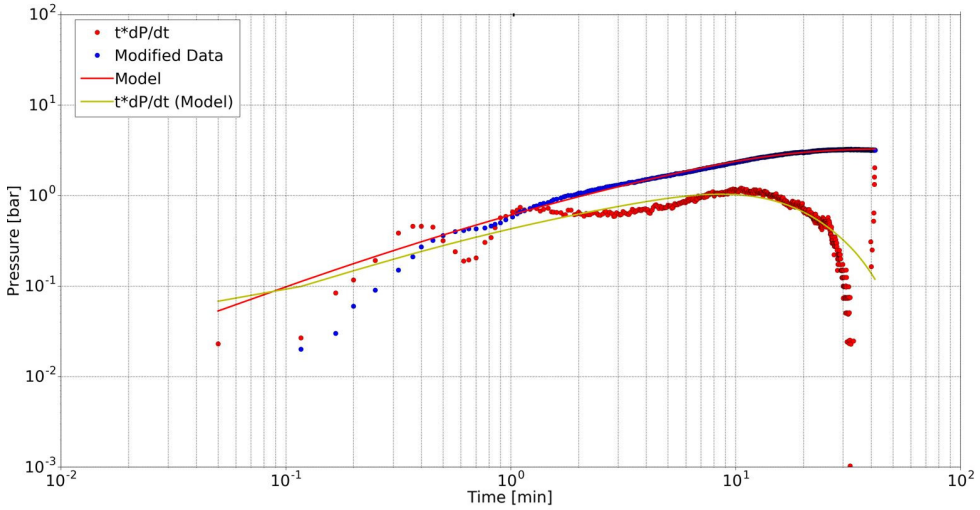

FIGURE 21: The modelling result of the third step of the second multistage injection test (March 2nd, 2016)

The pressure tool was lowered to a depth of 2200 m TVD. The production test was begun by controlling the valve opening with an initial opening of 65%, and then decrease to 46%, and further to 26%, and lastly, it was increased again to 65%. The initial opening of 65% corresponded to a discharge flowrate of 46.5 kg/s and downhole pressure of 147.39 bar, the 46% opening corresponded to 37.1 kg/s flow rate and downhole pressure of 147.84 bar. The 26% opening corresponded to a flowrate of 22.8 kg/s and a downhole pressure of 148.25 bar and the last opening of 65% corresponded to a flowrate of 24.3 kg/s and a pressure of 147.5 bar. All pressure measurements were plotted against time as Figure 22 shows.

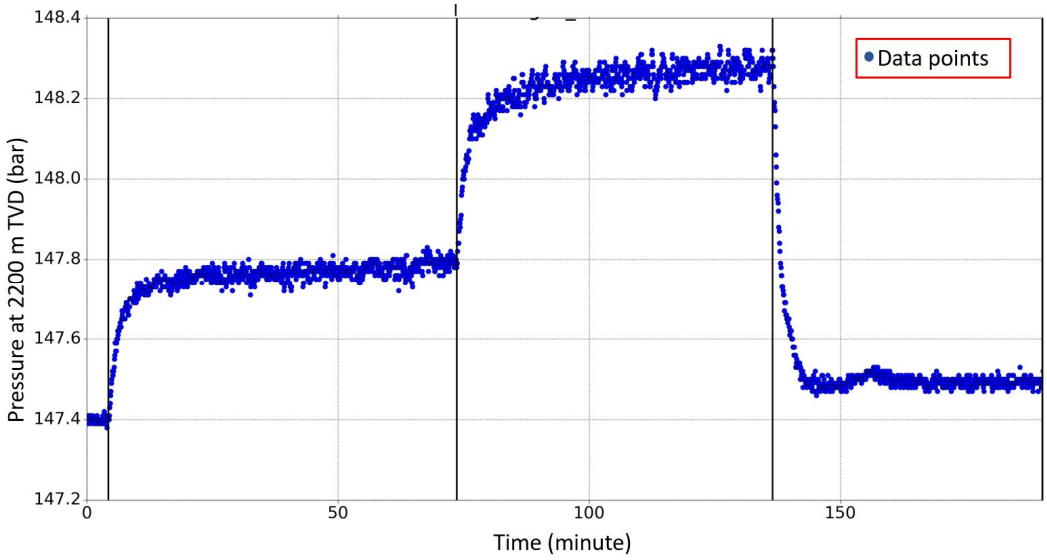

FIGURE 22: Multistage production test (May 17th, 2017)

The same method was applied as for the injectivity tests, where the stabilized pressure was plotted against the production flow rate and a linear trend line with its equation are generated from the graph. As shown in Figure 23, the resulting equation is y = -28.646x + 4270.6. It should be noted here, that the negative value in the generated equation means that it has opposite direction to the injectivity test which means that a certain amount of mass was extracted from the system. The productivity index value is then concluded to be 28.6 kg/s/bar.

The multistage productivity test was also modelled with the *Welltester* program to obtained reservoir properties. The same method as for the injectivity modelling was used with some reservoir properties

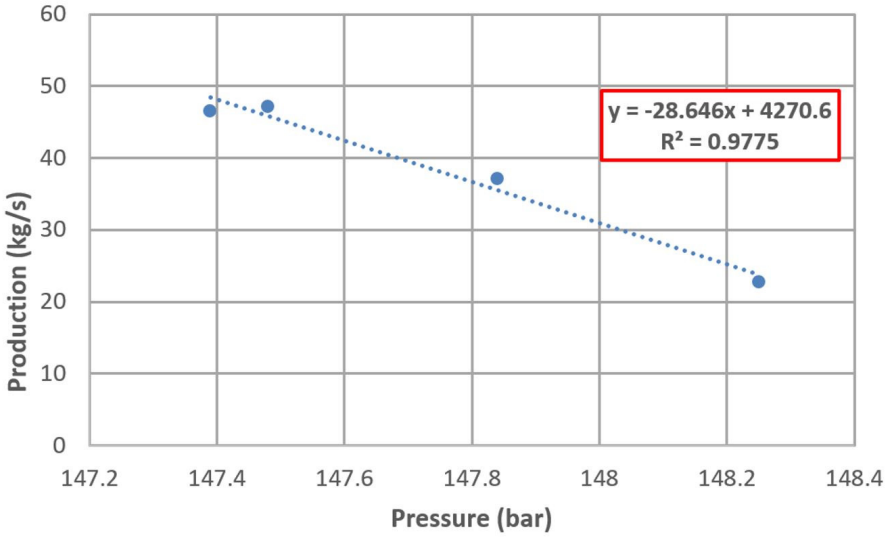

FIGURE 23: Productivity index estimation of well SV-26 based on the first multistage production test (May 17th, 2017)

introduced as initial value. However, one difference should be noted, which is that when choosing the type of test, production should be chosen instead of injection. As can be seen in Figure 22, the measurement result is rather scattered because the accuracy of the measurement device is not sensitive enough to measure such little differences in pressure, which is why some measurement points should be omitted before the modelling. The same type of reservoir conditions were also chosen for the modelling, with homogenous porosity, constant pressure boundary, constant wellbore storage and constant skin value. The graphs obtained from the modelling are shown in Figures 24-26 for the first, second and third step respectively. The parameters obtained are shown in Table 4 together with the results from previous modelling.

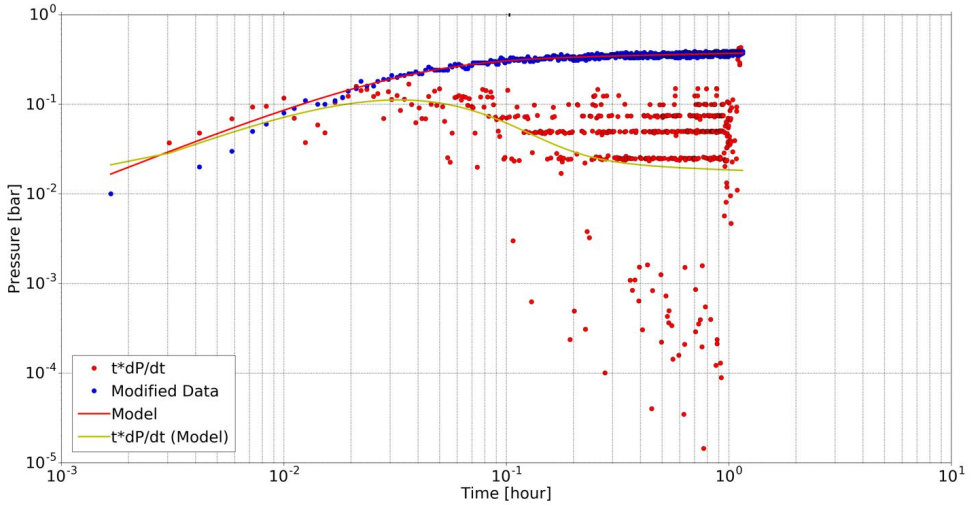

FIGURE 24: The modelling result of the first step of the multistage production test (May 17th, 2017)

5.4 Hydrological model summary

The first multistage injection test modelling resulted in an average injectivity index of 25.35 kg/s/bar, which is quite different from the linear model estimation of 14.3 kg/s/bar. However, as shown in Table 4, the second step is actually the one that has a very high value for the injectivity index (33.6 kg/s/bar) compared to the first step (17.1 kg/s/bar). The modelling result for the first injectivity index does not

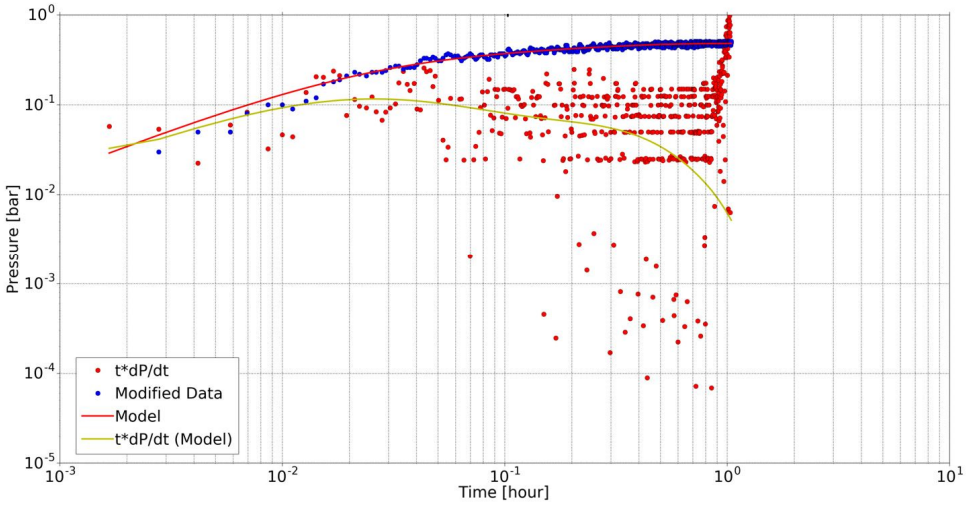

FIGURE 25: The modelling result of the second step of the multistage production test (May 17th, 2017)

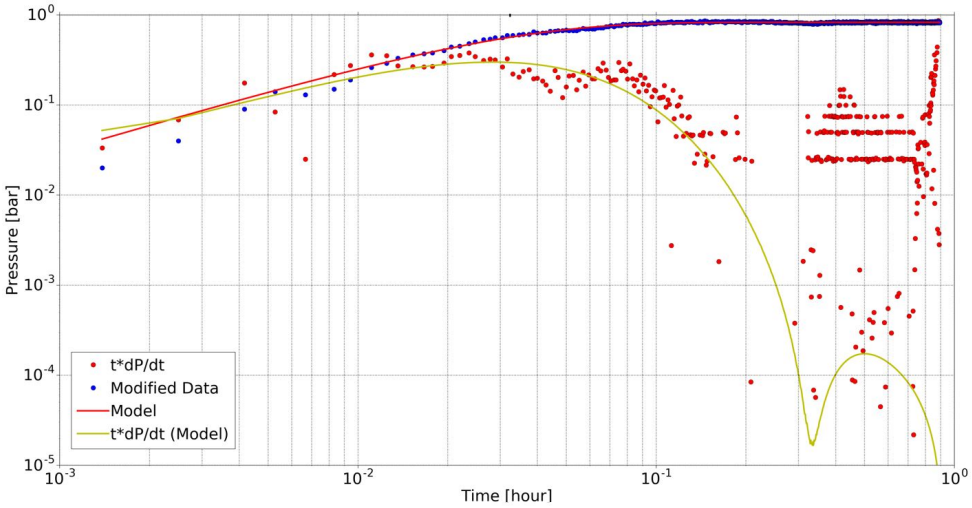

FIGURE 26: The modelling result of the third step of the multistage production test (May 17th, 2017)

really give a satisfying result as the coefficient of variation (CV) of the result is very high. This may be the result of a disturbed pressure measurement due to temperature changes in the well due to stimulation.

Unlike the first injectivity test, the average injectivity index from the *Welltester* program for the second multistage injection test is 10.8 kg/s/bar and gives a similar result to the previous linear model estimation, which is 11.4 kg/s/bar. The first step gives rather different values compared to the later steps especially for the storativity, reservoir thickness and effective permeability, but the first step also has very high values of CVs, which is why one should focus more on the result of the second and third step.

The transmissivity of all steps in the second injectivity test gives the value in order of 10^{-8}, which is very common for Icelandic geothermal reservoirs. The storativity value of the second and the third step also shows values in order of 10^{-8} which is common for liquid-dominated geothermal reservoirs, while two-phase reservoirs give values in order of 10^{-5} (Haraldsdóttir, 2009). The effective permeability of the second and third step also resulted in the value order of 10^{-14} and 10^{-15} (10 and 1 mD (milli-Darcy)), respectively. The first injectivity test shows an effective permeability in the degree of 1000 mD, which is much higher than in the second test. The difference may be because the 7" slotted liner had not yet been run into the well during the first test.

The skin values point to more negative values with more steps meaning that well is actually cleaned with more injection because it removes all the cutting and drilling mud that might block the feedzones to the reservoir. The well's best feedzones furthermore appear of fault origin due to the negative skin.

The multistage production test modelling resulted in an average productivity index of 28.11 kg/s/bar which is similar to the previous estimation of 28.6 kg/s/bar. Comparing to the second injectivity test, which was conducted in the same feedzone, the modelling result also gives quite similar results. For example, the effective permeability also gives result in order of 10^{-14} and 10^{-15} m^2 (10 and 1 mD) while the transmissivity and the storativity have higher values. This might be due to the yearlong interval between the second injection test and the productivity test that gives the well time to heat up. The higher productivity index compared to the injectivity index may also be affected by the slotted liner holes viscosity effect. This means that when the well is colder, the injected well fluid is off lower viscosity, which makes it more difficult to pass the liner holes. And vice versa, when the well is hot the low viscosity formation fluid will flow more easily through the liner holes than when cold.

6. WELLBORE SIMULATION

In this section, a wellbore simulation will be conducted for well SV-26 in Svartsengi, SW-Iceland to generate an output deliverability curve, as well as to estimate the relative contribution of the two major feedzones in the well. As discussed in Section 3, two major feedzones are found in the well at 1225 and 2200 m TVD. A multistage injectivity test was conducted on February 28th, 2016 in the shallow feedzone, with another one being done on March 2nd 2016 in the deep feedzone of the well. This was followed up with a multistage production test carried out on May 17th, 2017 in the deep part of the well. The reason for the tests was to estimate the feedzone properties as previously discussed in Section 4.

The wellbore simulation was conducted with the *Hola* program, developed by Björnsson et al. (1993), with parameters including the well design, the reservoir and well properties and most importantly the estimated feedzone properties of the well. In this simulation, radial heat loss by conduction between well and the ambient will be ignored.

The input parameters for the program were obtained from the previous sections of this paper. Some parameters have to be guessed and changed by trial and error by comparing the result with the measured data from the well. The measured data, which will be used for trial and error, are the data obtained from the multistage productivity test as shown in Table 5.

TABLE 5: Result of multistage productivity tests in SV-26

Parameters	Flowrate (kg/s)	Bottom pressure (bar)	Wellhead pressure (bar)
Initial	46.5	147.4	13.8
Step 1	37.1	147.8	13.8
Step 2	22.8	148.3	13.8
Step 3	47.1	147.5	13.7

Several attempts of trial and error were conducted by changing the feedzone parameters, especially the ratio of the productivity of the shallow and the bottom feedzones of the well. The ratios of productivity between the shallow and the deep feedzones tried were 1:1, 1:2, 2:1 and 2.5:1. The results of the productivity index and output deliverability are shown in Figures 27-30 for the respective productivity ratios.

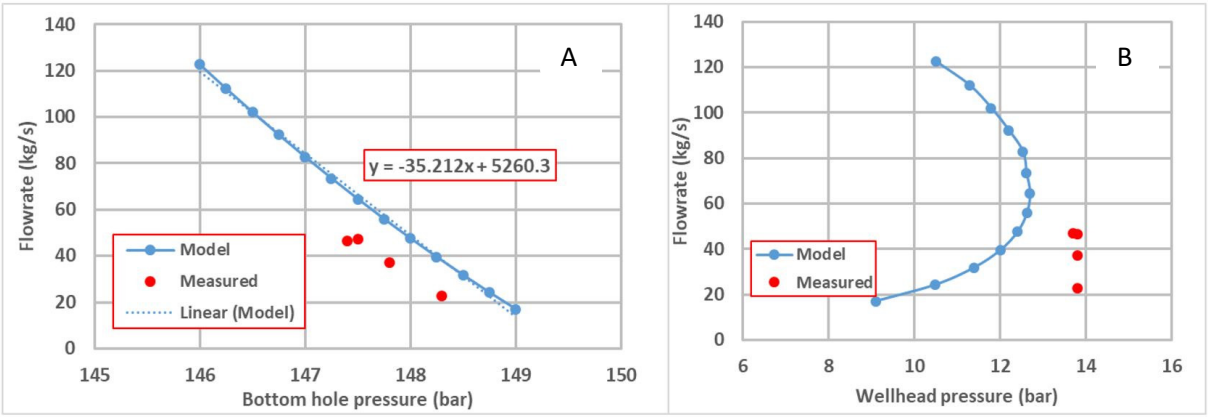

FIGURE 27: SV-26; a) Bottom hole pressure vs. discharge flowrate;
b) Wellhead pressure vs. discharge flowrate result from ratio of shallow and deep feed zone of 1:1

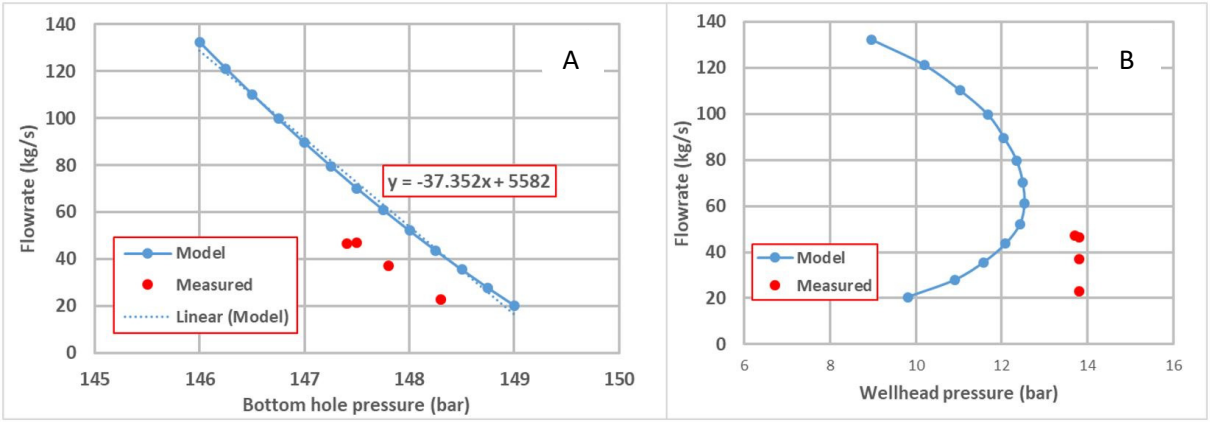

FIGURE 28: SV-26; a) Bottom hole pressure vs. discharge flowrate;
b) Wellhead pressure vs. discharge flowrate result from ratio of shallow and deep feed zone of 1:2

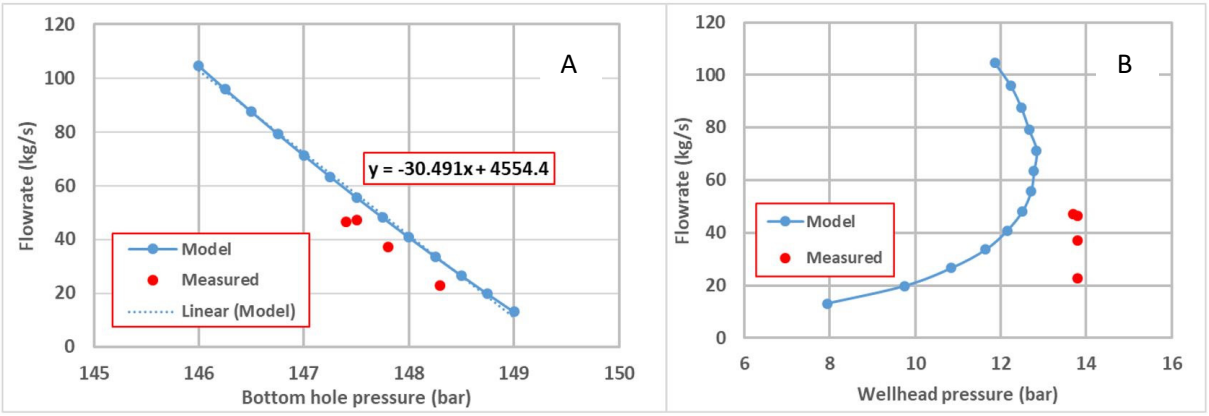

FIGURE 29: SV-26; a) Bottom hole pressure vs. discharge flowrate;
b) Wellhead pressure vs. discharge flowrate result from ratio of shallow and deep feed zone of 2:1

All of the figures above, especially the productivity of bottomhole pressure, were compared with the productivity index that was previously estimated as shown in Figure 23. In the figure, the resulting productivity index is 28.7 kg/s/bar. Comparing with the bottom hole pressure vs. flowrate results that

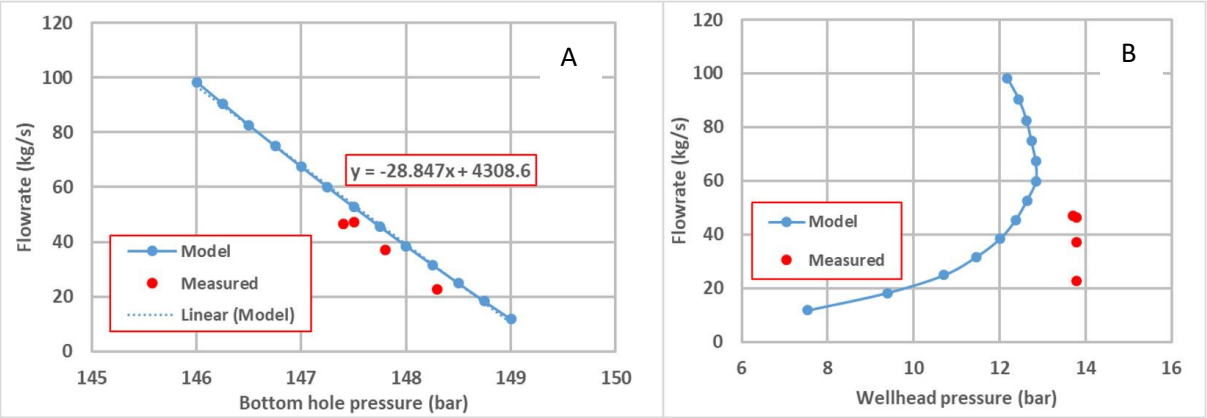

FIGURE 30: SV-26; a) Bottom hole pressure vs. discharge flowrate; b) Wellhead pressure vs. discharge flowrate result from ratio of shallow and deep feed zone of 2.5:1

are generated from the HOLA program, the 4th trial with a ratio of 2.5:1 between productivity of shallow and deep feedzone gives the best result with a productivity index of 28.9 kg/s/bar.

Generating the output deliverability curve that fits the model perfectly is a delicate process. The measured wellhead pressure of the well produces a variety of discharge flowrates with only small changes in wellhead pressure, which means that the well and reservoir have a very good permeability. The assumption of good permeability of the reservoir is also supported with the fact that the change of the bottomhole pressure is very small with the different discharge flowrates. The almost vertical measured wellhead output curve is rather hard to be fitted with trial and error by the *Hola* program despite changing various parameters such as the ratio feedzone productivity indices, enthalpy of the reservoir fluid and even the type of velocity method provided in the *Hola* program (Björnsson, et al., 1993). The best fitted result from the program is for the ratio of productivity of 2.5:1 between shallow and deep feedzones as it produces the closest values with the measured values as well as resulting in the most vertical curve compared to the others.

The almost vertical wellhead output curve also means that the well can actually deliver much higher flowrate than the maximum measured flowrate of 47 kg/s. In Figure 30, which shows the best model, the well can produce at a flowrate of 100 kg/s of reservoir fluid with a wellhead pressure of 12 bar. Assuming 20% dryness and a conversion of steam to power of 2 kg/s/MWe, the well can produce 10 MWe of electricity.

After the best ratio of productivity is obtained, the resulting modelling data and the measured data for dynamic pressure and temperature with depth are plotted with the HOLA program. The resulting plot is shown in Figure 31 together with the well design and the mass contribution of each feedzone. From the plot we can see that the flowrate contribution of the shallow and the deep zone is 30.7 kg/s and 14.9 kg/s, respectively, or about 2:1. The end result of ratio of mass flowrate gives a rather different ratio than those of the productivity of the feedzone. This is because the mass flowrate contribution is not only controlled by the productivity of the feedzone but also the difference between the pressure of the reservoir and the well.

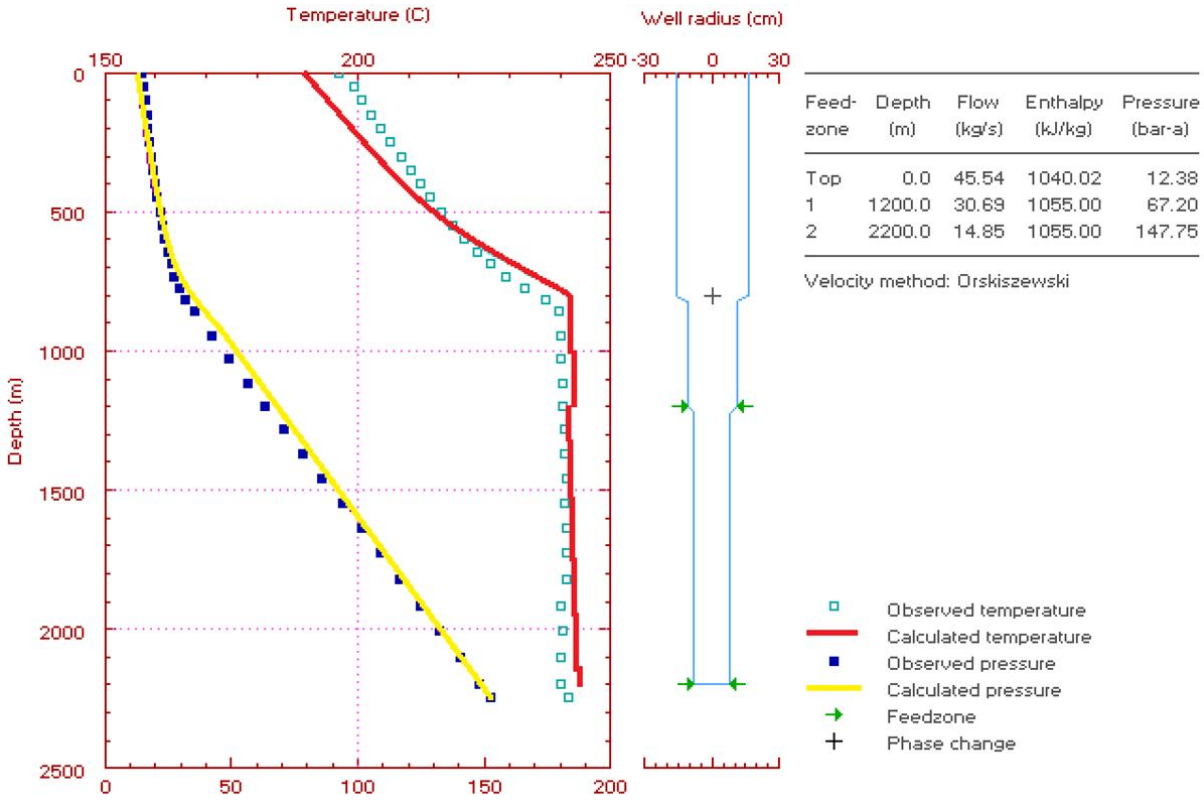

FIGURE 31: Measured and modelled pressure and temperature data from the production test

7. CONCLUSIONS

The volumetric assessment of a geothermal reservoir can be conducted in different stages of its development. An attempt to estimate the geothermal reserves was conducted for Corbetti, Ethiopia, which is currently in the early development stage and for Rantau Dedap, Indonesia, which has already delineated its potential through exploration drillings.

Volumetric assessment in Corbetti was made based on surface exploration surveys such as geology and geophysics to determine the reservoir surface area and thickness, while geochemistry was used to estimate the reservoir temperature. The estimation shows a P90 of 970 MWe and P50 of 1330 MWe.

In the Rantau Dedap area, the reserve estimation was based on more dependable data because downhole measurements had already been conducted for six exploration wells. The result of the reserves assessment based on a more developed data is usually smaller than that based on early exploration stage as the development progress has usually excluded area that is not feasible for development. In Rantau Dedap the reserves estimation in this paper resulted in a P90 of 49.3 MWe and a P50 of 82.0 MWe, which is much smaller than the earlier estimation of 220 MWe stated in the Geothermal Working Area tender document of Rantau Dedap. An attempt to utilize more energy is made by applying a bottoming system in the power plant, which in this study resulted in additional capacity of a P90 of 25.9 MWe and P50 42.3 MWe by applying a binary cycle.

Downhole temperature and pressure measurements are one of the most important tools for predicting reservoir parameters, which will be used for the next development stage, resource assessment and modelling of the reservoir system. In this paper, interpretation of downhole pressure and temperature logging was conducted for well SV-26 in Svartsengi, SW-Iceland while the well was being drilled,

injected, static and in discharge. From the logging analysis, one can obtain a lot of information. This includes the location of major feedzones, which are at 1225 and 2200 m TVD, the location of the static water table, which is at 425 m TVD, the location where the reservoir fluid starts to boil, which is around 700 m TVD, the pivot point location at 1350 m TVD, which corresponds to 77 bar reservoir pressure, and also initial temperature, which is predicted to be around 240°C.

Injection and production tests were conducted to estimate the injectivity and the productivity of the well as well as other reservoir parameters. Two injection tests and one production test, which were conducted in well SV-26 were modelled with the *Welltester* program. The average injectivity index for the first injection test was 25.4 kg/s/bar, while the average injectivity index for the second test was 10.8 kg/s/bar and the average productivity index was 28.1 kg/s/bar. From the analysis of coefficient of variation (CV) in the modelling results, the second injectivity test, especially the second and the third step, and the productivity test give the best fit to the measured data.

The high injectivity and production indexes indicate a very good reservoir permeability. The transmissivity of the reservoir based on the second injectivity test is on the order of 10^{-8} (m^3/Pa s) which is usual for geothermal reservoir in Iceland while the storativity is also on the order of 10^{-8}, which indicates a liquid-dominated reservoir. Both the transmissivity and the storativity are getting higher in the production test, which indicates the heating up of the well, with more steam gathering in the well. The skin value also points to more negative values within each step within an injection or production test, which indicates that the well is being stimulated and resulting in better permeability with more injection and production.

The wellbore simulation was conducted with the *Hola* program to generate the well output curve and to estimate the contribution of the feedzones in the well. The modelling was conducted with trial and error by changing the productivity ratio of the shallow and the deep feedzones of the well and try to fit it with the measured productivity from the bottom pressure and wellhead pressure. The best fit was generated from a productivity index ratio of 2.5:1 for the shallow and the deep feedzones, which resulted in a flowrate ratio of 2:1 between the shallow and the deep feedzones. The difference of the productivity and the resulting flowrate is due to other factors that also control the flowrate, for example the difference between reservoir pressure and well pressure. The resulting, almost vertical wellhead output curve suggests that the well can produce at a high flowrate of up to 100 kg/s. Assuming a dryness of 20% and a steam to power conversion of 2 kg/s/MWe, the capacity of the well is 10 MWe.

ACKNOWLEDGEMENTS

First of all, I would like to express my sincerest gratitude to Mr. Grímur Björnsson and Mr. Gunnar Thorgilsson as the supervisors of this project, who have helped me through their guidance, exciting discussion and astounding transfer of knowledge.

I would also like to extend my heartfelt appreciation to the UNU-GTP director, Mr. Lúdvík S. Georgsson, who has given me this tremendous opportunity to participate in this training. Many thanks also to the UNU-GTP staff members Ms. Málfrídur Ómarsdóttir, Mr. Ingimar G. Haraldsson, Mr. Markús A.G. Wilde and Ms. Thórhildur Ísberg. This course has been one of the most fulfilling experiences in my life – thanks to you all. I would also like to thank all of the UNU-GTP lecturers that have brought me a lot of new things throughout this course, all of ÍSOR staffs, and Orkustofnun staffs that have helped me during my study. Thank you also my new family, all of the UNU fellows of 2017.

I would like to express my profound gratitude to the Director of Geothermal, Mr. Yunus Saefulhak and all of my colleagues in the Directorate of Geothermal, MEMR, who have supported and helped me all this time. I would also thank the Supreme Energy team, who have helped me by providing data for this

project. And my special thanks to Dr. Havidh Nazif, who has supported and encouraged me from the very beginning to participate in this training.

And finally, many thanks and love for my family who have always supported me to follow all of my hopes and dreams.

REFERENCES

Arason, T., Björnsson, G., Axelsson, G., Bjarnason, J.Ö., and Helgason, P., 2004: *Icebox: geothermal reservoir engineering software for Windows, a user´s manual.* ÍSOR – Icelandic GeoSurvey, Reykjavík, report ÍSOR -2004/014, 80 pp.

Bacquet, A., Putra, A.P., Björnsson, G., and Arnaldsson, A., 2016: Inverse numerical modelling of Rantau Dedap geothermal field after six exploration wells. *Proceedings of the 41st Workshop on Geothermal Reservoir Engineering, Stanford, Ca.* 1-12.

Björnsson, G., Arason, P., and Bödvarsson, G.S., 1993: *The wellbore simulator HOLA. Version 3.1. User's guide.* Orkustofnun, Reykjavík, 36 pp.

Björnsson, G., and Novianto, 2015: *Analysis of downhole temperature and pressure data in Rantau Dedap and the conceptual reservoir model*. PT Supreme Energy, unpublished report, 30 pp.

Björnsson, G., and Steingrímsson, B., 1992: Fifteen years of temperature and pressure monitoring in the Svartsengi high-temperature geothermal field in S-W Iceland. *Geothermal Resources Council, Transactions, 16*, 627-633.

ChemicaLogic, 2018: *SteamTab, thermodynamic and transport properties of water and steam. Spreadsheet add-in software*. ChemicaLogin, Corp.: website: *www.chemicalogic.com/Pages/SteamTab.html*

Cumming, W., 2016: Resource capacity estimation using lognormal power density from producing fields and area from resource conceptual models: advantages, pitfalls and remedies. *Proceedings of the 41st Workshop on Geothermal Reservoir Engineering, Stanford, Ca.* 8 pp.

Dickson, M.H., and Fanelli, M., 2004: *What is geothermal energy?* International Geothermal Association, website: *iga.igg.cnr.it/geo/geoenergy.php.*

Fridleifsson, G.Ó., and Elders, W.A., 2017: The Iceland Deep Drilling Project geothermal well at Reykjanes successfully reaches its supercritical target. *Geothermal Resources Council, Bulletin, March/April 2017,* 30-33.

Georgsson, L.S., 2017: *Geothermal energy in the world - present status and future predictions*. UNU-GTP, Iceland, unpublished lecture notes.

Gíslason, G., Eysteinsson, H., Björnsson, G., and Hardardóttir, V., 2015: Results of surface exploration in the Corbetti geothermal area, Ethiopia. *Proceedings of the World Geothermal Congress 2015*, *Melbourne, Australia,* 10 pp.

Grant, M.A., and Bixley, P.F., 2011: *Geothermal reservoir engineering* (2nd ed.). Academic Press, MA, 288 pp.

Grant, M.A., Donaldson, I.G., and Bixley, P.F., 1982: *Geothermal reservoir engineering*. Academic Press, NY, 359 pp.

Haraldsdóttir, S.H., 2009: *Well testing report for well HE-29, Hellisheidi*. ÍSOR - Iceland GeoSurvey, unpublished report, 24 pp.

Haraldsdóttir, S.H., 2017: *Well testing theory - injection*. UNU-GTP, unpublished lecture notes.

Horne, R.N., 1995*: Modern well test analysis* (2nd ed.). Petroway, Inc., Palo Alto, Ca, 257 pp.

Humaedi, M.T., Alfiady, Putra, A.P., Martikno, R., and Situmorang, J., 2016: A comprehensive well testing implementation during exploration phase in Rantau Dedap, Indonesia. *Proceedings of the 41st Workshop on Geothermal Reservoir Engineering, Stanford University, Stanford, CA*, 10 pp.

Kutasov, I.M., and Eppelbaum, L.V., 2005: An improved Horner method for determination of formation temperature. *Proceedings of the World Geothermal Congress 2005*, *Antalya, Turkey,* 4 pp.

Marteinsson, K., 2017: *Introduction to Berghitti*. UNU-GTP, unpublished lecture notes.

Ministry of Energy and Mineral Resources, 2017: *Geothermal investment opportunities in Indonesia*. Directorate of Geothermal, Directorate General of New, Renewable Energy and Energy Conservation, Ministry of Energy and Mineral Resources, Jakarta, Indonesia, 142 pp.

Missouri University of Science and Technology, 2011: *Monte Carlo simulation in probabilistic engineering design. MUST, Mo, US,* 18 pp.

Moon, H., and Zarrouk, S.J., 2012: Efficiency of geothermal power plants: a worldwide review. *Proceeding of the 32nd New Zealand Geothermal Workshop, Auckland, NZ*, 13 pp.

Muffler, P., and Cataldi, R., 1978: Methods for regional assessment of geothermal resources. *Geothermics, 7*, 53-89.

PT. Supreme Energy Rantau Dedap, 2015: *Geoscience survey and drilling report of Rantau Dedap area (in Bahasa Indonesia).* PT. Supreme Energy Rantau Dedap, unpublished report, 29 pp.

Raychaudhuri, S., 2008: Introduction to Monte Carlo simulation. *Proceedings of the 2008 Winter Simulation Conference*, *Miami, Fl,* 91-100.

Sarmiento, Z.F., and Björnsson, G., 2007: Geothermal resource assessment – volumetric reserves estimation and numerical modelling. *Presented at "Short Course on Geothermal Development in Central America – Resource Assessment and Environmental Management", organized by UNU-GTP and LaGeo, San Salvador, El Salvador*, 6 pp.

Sarmiento, Z.F., Steingrímsson, B., and Axelsson, G., 2013: Volumetric resource assessment. *Presented at "Short Course on Surface Exploration for Geothermal Resources", organized by UNU-GTP and LaGeo, Santa Tecla, El Salvador*, 10 pp.

The World Bank, 2017: *Indonesia: geothermal energy upstream development project.* The World Bank, website: *projects.worldbank.org.*

Thorgilsson, G., Óskarsson, F., and Gudmundsdóttir, V., 2017: *Svartsengi – well SV-26 discharge testing on May 17th 2017*. ÍSOR – Icelandic GeoSurvey, unpublished report, 37 pp.

Tri Handoko, B., 2010*: Resource assessment of Tompaso geothermal field, Indonesia*. Report 30 in: *Geothermal training in Iceland 2010*. UNU GTP, Iceland, 647-674.
Tulinius, H., 2017: *Conceptual models of geothermal systems*. UNU-GTP, unpublished lecture notes.

Weisenberger, T.B., Gudjónsdóttir, S.R., Tryggvason, H., Hardarson, B.S., Gunnarsdóttir, S.H., Níelsson, S., Sigurgeirsson, M.A., Einarsson, G.M., Kristinsson, B., Pétursson, F., Ingólfsson, H., Stefánsson, H.O., Jónasson, H., Tulinius, H., and Gunnarsson, B.S., 2016: *Well report – SV-26 drilling of well SV-26 in Svartsengi from surface down to 2537 m and geothermal studies during drilling of the well*. ÍSOR – Iceland GeoSurvey, report 2016/022, 140 pp.

WestJEC, 2016: *Aluto-Langano resource assessment report*. Ethiopan Electric Company and West Japan Engineering Consultants, Inc., unpublished report, 238 pp.